SYNTHESIS AND REINFORCEMENT OF PEROXIDE-CURED BUTYL RUBBER THERMOSETS

by

Antonio Cillero Rodrigo

A thesis submitted to the Department of Chemical Engineering

In conformity with the requirements for

the degree of Master of Applied Science

Queen's University

Kingston, Ontario, Canada

(November, 2014)

Abstract

Isobutylene-rich elastomers provide the oxidative stability and impermeability required by many industrial applications. Halogenated derivatives support a wide range of chemical modification processes that can overcome most performance limitations. This research involves the modification of brominated butyl rubber (BIIR) to introduce peroxide-curable functionality in addition to aminotrialkoxysilyl groups that improve interactions with siliceous fillers, and anthraquinone functionality that serves as a polymer-bound chromophore. The thesis also describes detailed studies of the influence of counter anions on imidazolium ionomer derivatives of brominated poly(isobutylene-co-p-methylstyrene) (BIMS). Exchanging bromide with dodecyl sulfate, styrene sulfonate and montmorillonite clay platelets provided new ionomer thermosets whose rheological, tensile and adhesive properties varied considerably from their parent material.

Acknowledgements

I would like to thank my supervisor, Professor J. Scott Parent, for his encouragement, support and guidance. I would also like to thank Professor Ralph Whitney for sharing his knowledge and expertise freely throughout this project.

I am indebted to the following people for the valuable technical assistant provided over the course of this research project. Steven Hodgson and Kelly Sedore for their technical support with the equipment on the pilot plant; Kalam Mir for the training on the use of the UV-vis spectrophotometer and the DSC instrument; Dr. Francoise Sauriol for her assistance in interpreting my NMR spectra; Agatha Dobosz for helping me conduct XRD analysis on polymer nanocomposite samples; and all members of the Parent research group, Monique, Chris, Jackson, Brian and David, for their continuous help and advice. A final heartfelt thanks go to Professor Barrie Jackson, without whom I would not have pursued a Master's degree at Queen's University.

Financial support from Queen's is gratefully acknowledged. Materials provided by LANXESS and Exxon Mobil are also greatly appreciated.

Table of Contents

List of Figures

List of Tables

List of Abbreviations

PIB	Polyisobutylene
IIR	Poly(isobutylene-co-isoprene) or butyl rubber
XIIR	Halogenated butyl rubber
BIIR	Brominated butyl rubber
BIMS	Brominated poly(isobutylene-co-para-methylstyrene)
G'	Storage Modulus
G''	Loss Modulus
tan δ	Loss Tangent
T_g	Glass Transition Temperature
IIR-DDI	IIR-g-dodecyl itaconate
IIR-ASI	IIR-g-aminopropyltriethoxysillane
IIR-AAI	IIR-g-itaconamido anthraquinone
AA	1-amino anthraquinone
AAI	1-itaconamido anthraquinone
NMR	Nuclear Magnetic Resonance
THF	Tetrahydrofuran
DCP	Dicumyl Peroxide
DSC	Differential Scanning Calorimetry
IMSVImBr	IMS-vinylimidazolium bromide
IMSBuImBr	IMS-butylimidazolium bromide
IMSVImDS	IMS-vinylimidazolium dodecyl sulfate
IMSBuImDS	IMS-butylimidazolium dodecyl sulfate
IMSVImSS	IMS-vinylimidazolium styrene sulfonate
IMSBuImSS	IMS-butylimidazolium bromide sulfonate
IMSDI	IMS-dodecylitaconate

Chapter 1

Introduction

1.1. The development of synthetic rubber

Polyisobutylene (PIB) is an elastomeric polymer that provides low permeability to small molecule penetrants (Boyd & Pant, 1991), good thermal and oxidative stability, low toxicity, and high tack (Kunal, et al., 2008). PIB was first synthesized in 1873 through cationic polymerization (Puskas & Kaszas, 2003), but the saturated, unreactive polymer could not be cross-linked, limiting its range of applications.

.

In 1929, a German scientist working for I.G. Farben invented Buna-S, a copolymer of butadiene and styrene which, at the time, proved to be the most suitable alternative to natural rubber. The properties of this polymer were far superior to other synthetic rubbers of the time, but major technical problems remained, which resulted in German tires lasting only a tenth as long as those made of the natural rubber used by the Allies, making rubber a strategic resource during the Second World War.

In the United States, a synthetic rubber called neoprene, a homopolymer of chloroprene, was produced by DuPont in 1932, but synthetic rubber could not yet match the flexibility, durability and strength of natural rubber. Furthermore, natural rubber was cheaper to produce, leaving no economic incentive to develop a full-scale synthetic rubber industry. In 1937, the Standard Oil Development Co. laboratories (now Exxon Chemical) developed butyl rubber (IIR) (C.A.S. No.9010-85-9), a copolymer of isobutylene and isoprene that displayed good thermal stability

along with some other industrially attractive properties such as air impermeability and cure reactivity.

However, by 1941, natural rubber still accounted for 99% of American rubber consumption. In 1942, with the occupation of the natural rubber plantations in South East Asia by Japanese forces, the production of synthetic rubber dramatically increased in the United States and by 1945 it already represented 85% of USA domestic use. Finally, in 1946, the "Cold Rubber" process was invented, an innovation that significantly increased the flexibility and tread wear of synthetic rubber tires, making synthetic rubber the dominant product in the market.

At present, world rubber usage is about 15 million metric tons a year, split between natural rubber (35%), styrene-butadiene rubber (18%), polybutadiene rubber and other specialty polymers such as urethanes, halogenated polymers, silicones and acrylates (47%) (Barbin & Rodgers, 2005).

1.2. Polyisobutylene, butyl rubber and their derivatives

Isobutylene-based polymers include polyisobutylene (PIB), copolymers of isobutylene and small amounts of isoprene known as butyl rubber (IIR), halogenated butyl rubber (XIIR, where X=Cl or Br) and brominated poly(isobutylene-co-para-methylstyrene) (BIMS) (Figure 1.1). Butyl rubber (IIR) is synthesized by the copolymerization of isobutylene and 1-2% isoprene through a carbocationic polymerization using Friedel-Crafts type Lewis acids at low temperature (Kennedy & Marechal, 1982). Some of the key features of butyl rubber and its derivatives are excellent thermal aging, good damping properties at room temperature, exceptional impermeability to air and moisture due to the close packing of the isobutylene chain segments, good flexibility at low temperature due to a low Tg, and good resistance to heat, chemical and oxidative degradation due

to their nearly saturated polymer backbone. Some of its deficiencies include low tensile strength, low adhesion, and poor sulfur vulcanization rate.

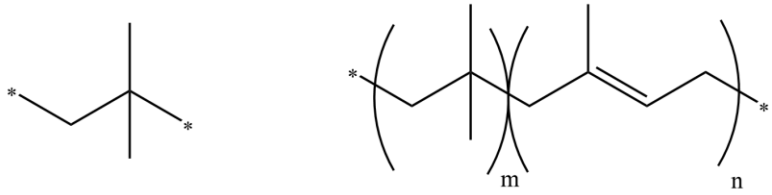

Polyisobutylene (PB) Poly(isobutylene-co-isoprene)/Butyl rubber (IIR)

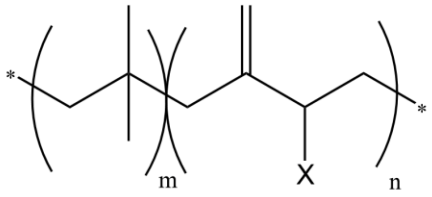

Halogenated butyl rubber (XIIR), X= Cl, Br

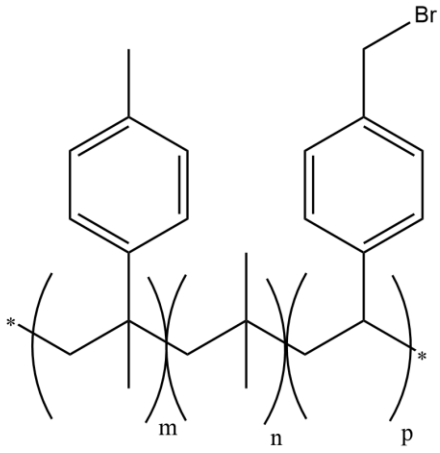

Brominated poly(isobutylene-co-paramethylstyrene) (BIMS)

Figure 1.1. Polyisobutylene and its isobutylene-rich copolymers

Butyl rubber is halogenated using Cl_2 or Br_2 in a multiphase continuous reactor. In the early 1960s, Exxon Chemical commercialized chlorobutyl rubber, whose allylic halide functionality improved reactivity in curative formulations containing elemental sulphur and metal oxides. In

today's marketplace, chlorobutyl and bromobutyl rubber remain the most important tire inner liner materials, owing to their good sulfur cure reactivity as well as the simplicity of the halogenation process. Note that IIR halogenation is an allylic substitution reaction, yielding two isomers, with the exomethylene isomer (structure 1 in Figure 1.2) generated as a kinetically favored product (Vukov, 1984).

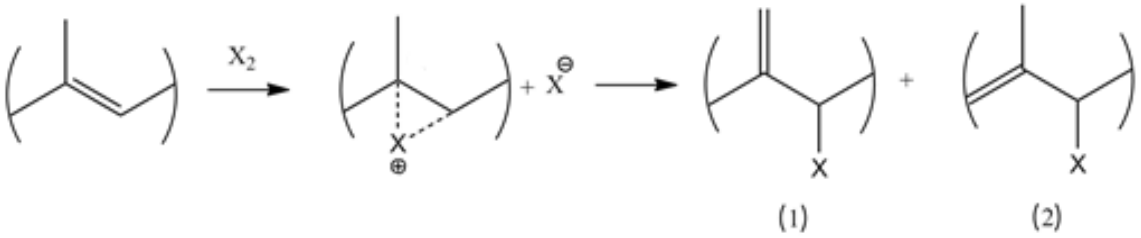

Figure 1.2. Reaction mechanism for the halogenation of IIR (Vukov, 1984).

Poly(isobutylene-co-p-methylstyrene) is prepared by copolymerization of para-methylstyrene with isobutylene via carbocationic copolymerization using strong Lewis acid initiators such as $AlCl_3$ at low temperature (Kaszas, 2001). Since the monomers have similar copolymerization reactivity ratios, the final composition of the rubber is close to the monomer feed ratio, and para-methylstyrene units are distributed more or less uniformly. This allows producers to prepare materials whose properties vary widely with para-methylstyrene monomer content, from polyisobutylene-like ozone-resistant elastomers to poly(para-methylstyrene)-like tough, glassy plastics. In addition, copolymers maintain some of the characteristics of the constituent homopolymers, with isobutylene-rich polymers providing low permeability and good dynamic response.

Benzylic bromide functionality can be introduced to poly(isobutylene-co-p-methylstyrene) by selective free-radical bromination on the *para*-methyl position using Br_2 and a radical initiator

(Figure 1.3) (Powers, et al., 1992). This electrophilic functional group can be easily converted by nucleophilic substitution, allowing for the introduction of additional pendant groups to a BIMS backbone.

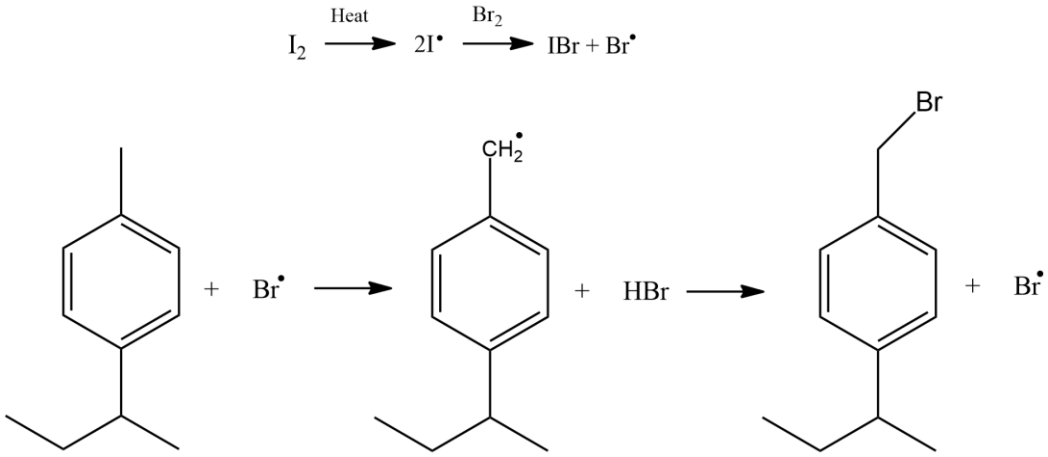

Figure 1.3. Bromination of poly(isobutylene-co-paramethylstyrene) (Powers, et al., 1992).

BIMS can be crosslinked using zinc oxide and multifunctional nucleophiles such as diamines. For example, BIMS has been used to produce tire curing bladders in conjunction with graphite fillers and 1,6-hexamethylene-bis(sodium thiosulfate) (HTS) using zinc oxide as the curing agent (Duvdevani & Frederick-Newman, 1997). However, BIMS cures extremely slowly with zinc oxide, which limits the number of applications and the range of cure formulations that can be used with this elastomer.

1.3. Peroxide curable derivatives of IIR and IMS

Uncrosslinked elastomers are amorphous materials that are used above their glass transition temperature, meaning that polymer chains have the ability to move past each other when subjected

to an applied stress. Since chain entanglements are their only mechanism to resist deformation, elastomers suffer from creep and/or stress relaxation to an extent that makes them unsuitable for most engineering applications. Crosslinking (also known as curing or vulcanization) is the process by which intermolecular covalent bonds are created so polymer chains can no longer flow freely (Coran, 2005) (Figure 1.4). According to the theory of rubber elasticity (Flory, 1953), retractive forces that resist deformation are proportional to the molecular weight of polymer segments between network junctures. Higher crosslink densities reduce this quantity, hindering polymer segment mobility, and increasing elasticity.

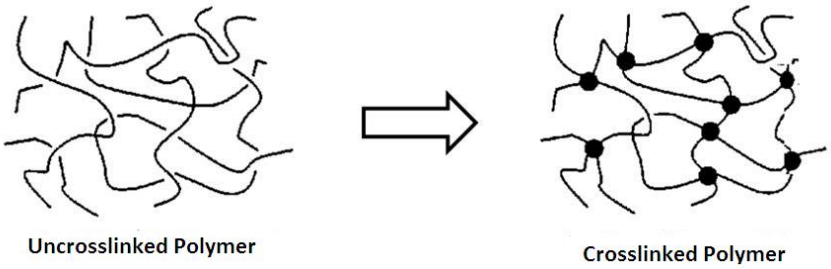

Figure 1.4. Schematic representation of a polymer crosslinked network (Coran, 2005)

When an oscillatory strain is applied to a viscoelastic material, the resulting stress has two components; one in-phase with the strain, giving the "storage modulus" (G') and one out-of-phase, giving the "loss modulus" (G'') (Brown, 2006). The storage modulus represents the energy recovered elastically during the cyclic deformation, and serves as a proxy for cross-link density, according to the kinetic theory of rubber (Auluck & Kothari, 1943). The loss modulus, on the other hand, is a measure of the energy dissipated as heat. In a typical controlled strain measurement, the applied strain is described by Equation 1.1, while the observed stress is given by Equation 1.2.

$$\gamma(t) = \gamma_0 \sin(\omega t) \qquad (1.1)$$

$$\sigma(t) = \gamma_0 \left[G'(\omega) \sin(\omega t) + G''(\omega) \cos(\omega t)\right] \qquad (1.2)$$

The elasticity of a material is often gauged by the ratio of the loss modulus to the storage modulus, which equals the tangent of the phase angle (δ), as expressed in Equation 1.3. An ideal elastic material has a tan δ equal to zero, while an ideal viscous liquid would have a tan δ approaching infinity (Brown, 2006).

$$\tan\delta = \frac{G''}{G'} \qquad (1.3)$$

There are two major commercial technologies for crosslinking rubber; sulfur cure formulations and peroxide cure formulations (Dluzneski, 2001). Sulfur vulcanization can only be applied to polymers that contain C=C unsaturation, but these materials generally provide superior dynamic properties, owing to the labile polysulfide crosslinks introduced by this cure chemistry. This process is widely used in butyl rubber and halobutyl rubber applications (Parent, et al., 2003).

The use of peroxides for crosslinking of elastomers has been known since 1915. However, peroxide crosslinking chemistry received little interest until saturated ethylene-propylene copolymers were introduced in the 1970s. There are a number of advantages associated to the use of peroxides for crosslinking, such as simple compound formulation, scorch-free storage of compounds, and the possibility of applying high crosslinking temperatures without reversion. Peroxide cures can function on both saturated and unsaturated polymers, but they are not universally applicable. For example, PIB does not crosslink when exposed to peroxides, since β-scission of macroradical intermediates leads to a decrease in molecular weight (Figure 1.5) (Thomas, 1961).

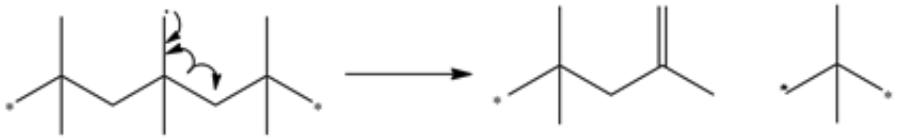

Figure 1.5. Chain scission of PIB

Commercial butyl rubber contains up to 2% of unsaturated isoprene mers, but this level of unsaturated monomer is not high enough to overcome degradation by chain scission, needing at least 3% isoprene content to do so (Loan, 1964). Increasing the isoprene content of IIR would favor peroxide crosslinking, but it would also compromise the oxidative stability of the polymer, leading to a reduction of long-term aging properties (Shaffer, et al., 2003). An alternate approach for generating peroxide-curable grades of butyl rubber involves chemical modification of BIIR. The introduction of acrylate (Xiao, et al., 2010) styrenic and maleimide groups (Kato, et al., 2006) supports crosslinking through radical oligomerization of pendant functionality.

These chemical modifications are bromide displacements from BIIR by the required carboxylate nucleophile. Note that the exomethylene isomer (Exo-Br, Figure 1.6) is the kinetically favored halogenation product but, unlike its E-BrMe and Z-BrMe isomers, it is not very reactive towards nucleophilic substitution (Parent, et al., 2010). The isomerization of the Exo-Br isomer to the more reactive E- and Z- isomers can be achieved by treatment with Lewis acids or bromide nucleophiles such as tetrabutylammonium bromide (TBAB) (Figure 1.6) (Malmberg, et al., 2010), giving a bromobutyl rubber derivative that reacts more rapidly than the starting material.

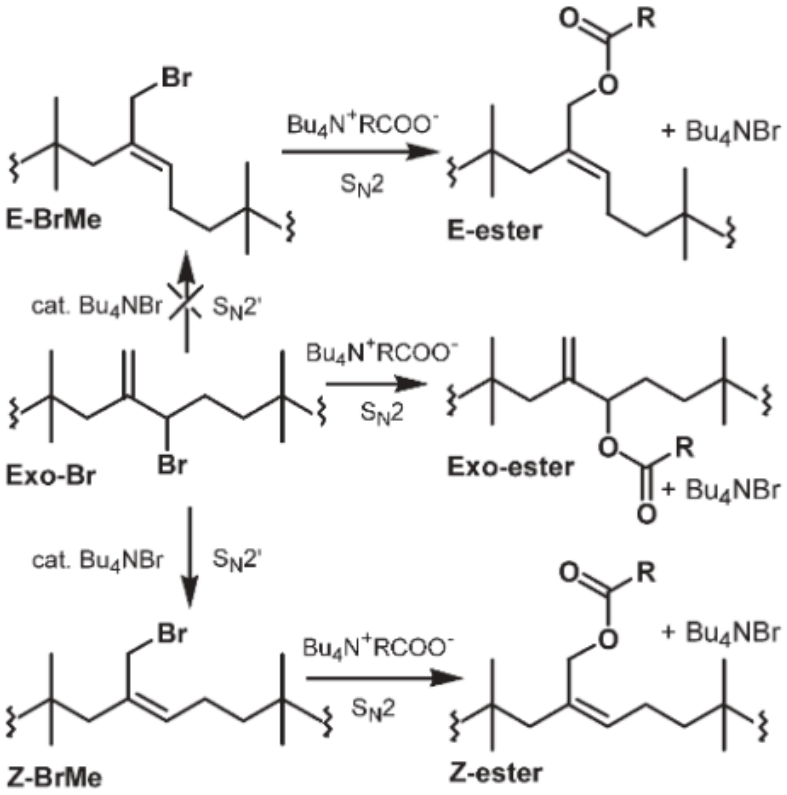

Figure 1.6. BIIR isomerization and esterification (Xiao, et al., 2010)

1.4. Ionomers

Ionomers are polymers containing small amounts of ionic groups (less than 15 mol %) attached to a hydrophobic backbone. Interacting forces between ionic groups modify some of the properties of the ionomer when compared to their non-ionic counterparts, such as dynamic mechanical properties, glass transition temperature, viscosity, melt strength and fatigue. Furthermore, ionic groups have shown to enhance adhesion to high energy surfaces (Resendes, et al., 2010) and improve interaction with polar fillers (Parent, et al., 2004). This wide range of possibilities makes ionomers a growing field of investigation, as proven by the number of papers published on the topic during the last fifty years.

The term “ionomer” was coined in 1965 by Rees and Vaughan to describe a class of thermoplastics (Surlyn®) comprised of ethylene mers with a small amount of partially neutralized methacylic acid groups distributed randomly within the polymer chain (Rees & Vaughan, 1965). Later, Eisenberg and Rinaudo proposed a definition for ionomers that stands until today; they described ionomers as polymers whose bulk properties are governed by ionic interactions in discrete regions of the material (Eisenberg & Rinaudo, 1990). According to the Eisenberg-Hird-Moore model (Eisenberg, et al., 1990), an ionic group can aggregate with other vicinal ionic groups to form the so-called “multiplets” (Figure 1.7). Multiplets are quadruplets, sextuplets or higher aggregates of ion pairs that act as thermo-reversible ionic cross-links between polymer chains. Most of the known multiplets show a spherically-like structure with the ion pairs oriented to the center of the sphere and the back-bone polymer chains oriented to the outside.

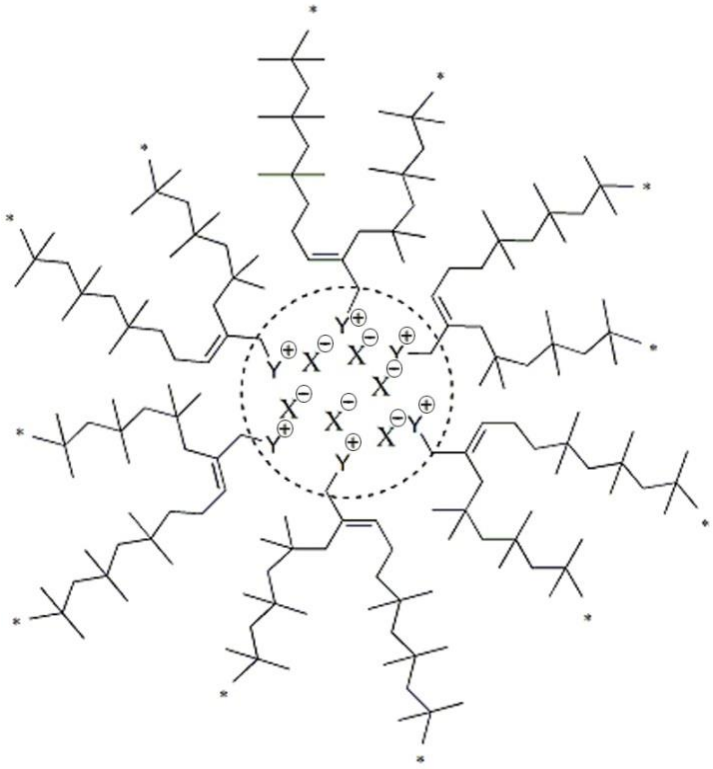

Figure 1.7. Schematic representation of a multiplet

Polymer chain segments attached to an ion pair that reside in a multiplet suffer reduced mobility, due to the anchorage of the ionic group. This yields two regions within a multiplet, "the core", formed by the actual ionic groups oriented to the center of the sphere, and "the skin", formed by the chains in the region of restricted mobility around the core. The thickness of "the skin" depends on the flexibility of the polymer backbone and the size of the core, and its magnitude determines some of the mechanical properties of the ionomer. The skin region tends to be thinner when the polymer chains attached to the ionic groups are flexible. On the other hand, the extent of mobility reduction is determined by the size of the multiplet; the larger the ion pair aggregate, the greater the number of polymer chains anchored to it and the greater the reduction of mobility (Eisenberg, et al., 1990). Formation of multiplets is determined by both the nature of the ionic

species and the nature of the host polymer. Additionally, ordered assemblies of multiplets in the solid state create clusters when their regions of restricted mobility merge. Ionic clusters undergo an order-disorder transition state at the cluster transition temperature (T_i). Aggregation between multiplets act as additional reversible cross-links and improve the mechanical properties of the ionomer.

The change observed in the glass transition temperature (T_g) between ionomers and their non-ionic counterparts clearly indicates the importance of ionic interactions in the mobility of polymer chains. It was found that the T_g of polyphosphoric acid increased from -10ºC to 280ºC when neutralized with Na^+ and up to 530ºC when it was neutralized with Ca^{2+} or Zn^{2+} (Eisenberg, et al., 1966). Similar behavior was observed for acrylate (Eisenberg, et al., 1971) and ionene ionomers (Eisenberg, et al., 1971).

1.5. Factors affecting multiplet formation

There are several parameters that affect the ionic aggregation, but the most influential are the proximity of ion pairs (determined by the ion content of the ionomer), the electrostatic interactions between ion pairs (determined by the nature of the ionic group and the counter ion) and the relative position of the ionic group within the polymer chain (whether they are attached to the main chain, to a side chain or to the backbone terminus).

Depending on the type of ionic groups and their distribution, there will be a minimum ion content for multiplet formation to occur. Ionomers containing high ion pair concentrations are more likely to produce nearest-neighbor interactions than those bearing small amounts of ionic functionality. The more ion groups are closer together, the better they can be incorporated into the

same multiplet. This leads to an enlargement of multiplet size which, in turn, promotes "ionic clustering" (Eisenberg & Kim, 1998).

The nature of the ionic group also determines the stability of the multiplets. At high temperature, migration of ion pairs between multiplets occurs, leading to a decrease in ionic interactions; this phenomenon is termed as "ion hopping" and it is characterized by a decrease in the observed modulus and, as a result, a downward trend in the ionic plateau. By comparing the temperature at which ion hopping occurs and the slope of the rubbery plateau, stability of multiplets for different ionomers can be established.

With respect to the nature of the ionic groups, several studies have shown significant differences between carboxylate and sulfonate ionomers. These materials are widely studied, owing to the ease of their synthesis and their versatility, which makes them useful for large scale production. Carboxylate anions can be incorporated to the polymer chain by copolymerization with methacrylic acid or maleic acid, among other unsaturated carboxylic acids, while sulfonated groups can be also incorporate to polymer chains by copolymerization or through sulfonation of a material post-polymerization.

According to the dynamic mechanical data obtained by some authors (Eisenberg & Hird, 1992), *para*-sulfonated polystyrene ionomers display an ionic plateau at ionic contents greater than 3.5 mol%. This plateau is the result of multiplets forming an ionic network that persists to temperatures that preclude "ion hopping". In comparison, p-carboxylate and methacrylate polystyrene ionomers show no ionic plateau, indicating that their multiplets are kinetically less stable. In addition, glass transition temperatures in sulfonated ionomers are higher than in their carboxylated counterparts, confirming that interactions between sulfonate groups are stronger than

those between carboxylate groups. It has also been observed that carboxylated polyurethane ionomers display lower tensile properties than the corresponding sulfonated ionomers, which again confirms the idea of the weaker strength of carboxylate interactions (Visser & Cooper, 1991).

Small-Angle X-ray Scattering (SAXS) is used to determine the size of nanoscale structures such as those of ionic multiplets. The Bragg distance that can be deduced from the peaks in a small-angle X-ray scattering analysis varies with the type of ionic group; this parameter can be considered as an indicative of the size of the ionic multiplet. Experimental data shows that *para*-carboxylate polystyrene ionomers show higher Bragg distances (~31 Å) than poly(styrene-co-methacrylate) ionomers (~23 Å) suggesting the presence of bigger multiplets on the former (Eisenberg & Hird, 1992). The difference in the ionic strength interactions between p-carboxylated and poly(styrene-co-methacrylate) is very low, so the source of multiplet size variation must be the position of the ionic group with respect to the polymer backbone. While the methacrylate group is forming part of the polymer backbone, the carboxylate group in the *para*-styrene position has a lower steric hindrance towards aggregation due to its separation from the backbone polymer chain.

Pendant ionic groups with stronger ionic interaction are energetically more favored to form multiplets than those which are attached directly to the polymer backbone. Although the size of a multiplet is limited by steric factors, geometric constrains limit the size of these ionic aggregations to a maximum diameter of around 6nm. Small, highly polar ion pairs are expected to interact more strongly with each other, leading to larger multiplets than ionomers with bigger ion pairs and weaker ionic strength (Eisenberg, et al., 1990).

Note that even though carboxylate multiplets are small, experimental tensile modulus values for these ionomers overcome the predicted values calculated by the rubber elasticity theory

(Eisenberg & Hird, 1992; Visser & Cooper, 1991). These studies suggest that due to the reduced size of the multiplets on these ionomers, they may act as fillers within the polymer matrix leading to the observed enhancement of the modulus. This explanation could also account the increase of the scope of this behavior with the increase of ion content of the polymer.

While studies (Eisenberg & Hird, 1992) of cesium, lithium and sodium sulfonate ionomers have suggested that the counter cation does not affect the aggregation of ion pairs into multiplets, work on alkali and alkaline earth metal salts of poly(ethylene-co-methacrylic acid) have shown significant differences in melting temperature, crystallization temperature, melt viscosity, tensile strength, thermal stability, and dynamic mechanical properties (Hirasawa, et al., 1991; Feldheim, et al., 1993; Gomes-Lage, et al., 2004). Cluster glass transition temperature and matrix glass transition temperature were considerably larger for alkali and alkaline earth ionomers than for transition metal ionomers, suggesting that strong interactions between alkali and alkaline earth ionic groups restrain polyethylene chain mobility. The type of counter cation and its concentration also affects the viscosity of the molten state, suggesting that ionic aggregation remains at elevated temperature.

Even greater variations in ionomer properties can be gained using counter ions other than metal salts. For example, sulfonated polystyrene neutralized with a series of alkyl amines displayed significantly different properties depending on the size of the organic base, suggesting that the increase in size of the counter cation reduces the strength of ion-dipole interactions within multiplets (Weiss, et al., 1984).

1.6. Ionomer derivatives of isobutylene-rich rubber

The first isobutylene-based ionomer reported in literature was a sulfonated isobutylene-based telechelic ionomer prepared by Tant et al. in 1985, which showed an increased in viscosity due to intermolecular association of the ionic groups (Tant, et al., 1985). However, interactions between ionic groups were labile and prone to relaxation when exposed to a static load (Bagrodia, et al., 1987). Crosslinking was therefore required to provide the physical properties needed for engineering applications. Many other butyl rubber-based ionomers have been synthesized since then, including some BIIR and BIMS ionomers synthesized by Parent et al. using tertiary amines, triphenylphosphine (Parent, et al., 2004) and azole functionality (Parent, et al., 2011) (Figure 1.8). These ionomers have shown improved adhesion to substrates whose surface has polar functional groups, good dispersion of siliceous filler (Parent, et al., 2004) and anti-microbial properties (Kleczek, 2013).

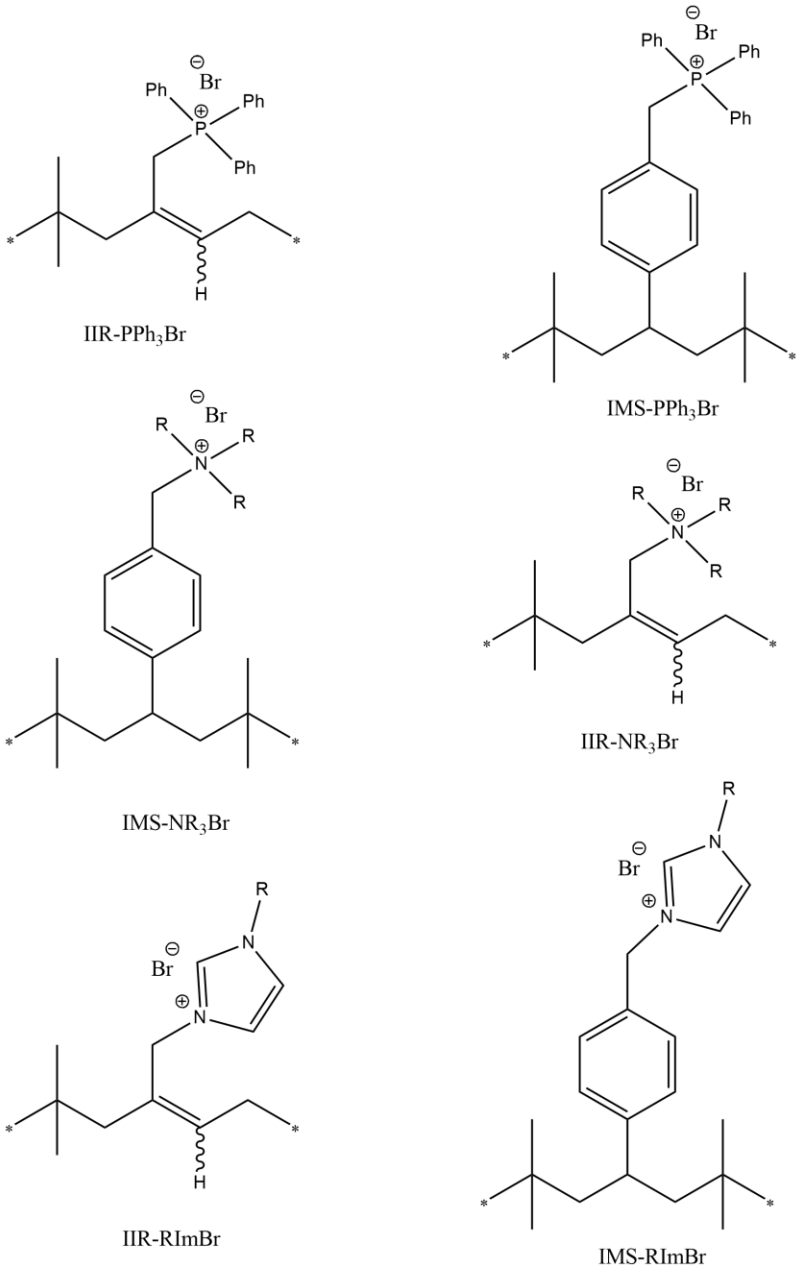

Figure 1.8. Ionomer derivatives of BIIR and BIMS

Tetraalkylammonium ionomers can be prepared from a wide variety of commercially available amines, but their lack of stability due to reversibility of the quaternization reaction reduces their range of application (Parent, et al., 2002; Gordon, 1965). Phosphonium and imidazolium

ionomers are attractive because of the ease of their synthesis in solvent-free conditions and their thermal stability (Parent, et al., 2011; Parent, et al., 2004), allowing them to be processed at the temperatures required for rubber compounding and crosslinking. Imidazole groups offer an additional technical advantage over phosphonium functionalities, the possibility of including additional pendant functionalities on their structure, such as peroxide-curable groups. These functional imidazoles containing unsaturated pendant groups allow for the manufacture of peroxide-curable ionomers that display reduced creep and stress relaxation.

1.7. Rubber Compounding

Compounding is a term that refers to the modification of an elastomer or a blend of polymers and other materials to meet material performance requirements. As an example, compounded rubber displays some unique characteristics such as good dampening properties, high elasticity and high abrasion resistance (Barbin & Rodgers, 2005).

Filled systems are those materials in which a filler or reinforcement, such as carbon black, silica or clay, is added to the rubber formulation to meet the target material properties. Carbon black is widely used as a filler in the tire industry and it has been found that carboxylic, phenolic, quinone, ketone and other functional groups on carbon black particle surface react with the polymer, resulting in better polymer-filler interactions (Le Bras & Papirer, 1979). However, its oil-based origin makes it a non-renewable filler and some of its components have been found to be carcinogenic (Heinrich, et al., 1994; Baan, et al., 2006).

Silica and clays are non-oil-based materials with considerable potential as fillers. Silica has weaker polymer-filler interactions and it is more difficult to disperse in non-polar elastomers due

to its high surface energy. Therefore, silane-coupling agents used in conjunction with intense dispersive mixing energy are required to achieve good polymer-filler interactions when using silica as a filler (Hopkins, et al., 2002).

Clay is one of the most widely used materials for the production of polymer nanocomposites due to its low cost, high availability and environmentally friendly properties. Conventional cationic clay minerals are formed by alumino-silicate sheets carrying a negative charge with cationic species in the interlayer between every two negatively charged layers. The most commonly used clays for the production of nanocomposites are from the smectite group of clays, from which one of the most important is montmorillonite (MMT), a clay with a cation exchange capacity of 0.9 mequiv./g of clay and a surface area of interlayer space of 54 m^2/g (Durán, et al., 2000).

Clay/polymer nanocomposites offer advantages over traditional filled composites at low filler loadings due to the nanometer scale of the clay platelets. But for many years, the main inconvenience when using clays as fillers was to break down clay particle aggregates into individual platelets to achieve good filler dispersion and exploit the potential reinforcement capacity of individual silicate layers. Polymer-clay nanocomposites based on layered alumino-silicates can be classified into three categories depending on the degree of exfoliation of the silicate layers in the polymeric matrix: tactoids, intercalated, and exfoliated. In tactoids, clay platelets are not exfoliated and there is phase separation between the big clay particles and the polymer matrix with the clay particles serving as conventional fillers. Intercalation occurs when a small amount of polymer penetrates into the gallery spacing between clay platelets expanding the interlayer spacing. Exfoliation occurs when clay platelets are significantly apart from each other due to extensive polymer penetration and the nanometer-thick clay platelets are distributed homogeneously through the polymer matrix.

In exfoliated nanocomposites the addition of clay does not significantly affect the optical properties of the polymer matrix due to the low thickness of the individual clay layers in comparison with that of conventional fillers. In addition, clay/polymer nanocomposites display other industrially attractive physical properties that include fire retardancy (Gilman, et al., 2000), enhanced barrier properties (Chang, et al., 2003; Gorrasi, et al., 2003) and ion conductivity (Kim, et al., 2008)

The use of ionomers or polyelectrolytes may provide an advantage in the dispersion of clay platelets due to the enhanced phase adhesion that can be achieved between the anionic clay platelets and the cationic groups of the polymer, improving the extent of reinforcement produced by the addition of clay. Despite that, very few studies have been conducted on the field of polymer/clay nanocomposites involving the use of polyelectrolytes or ionomers (Lee, et al., 2005; Xu, et al., 2006; Li, et al., 2010).

1.8. Objectives

The objectives of this study were:

- To graft peroxide-curable groups bearing additional functionalities of IIR and IMS and analyzed their mechanical and physical properties.
- To explore the impact of introducing different counter anions via anion metathesis on the properties of ionomeric derivatives of BIMS.

1.9. Works Cited

Auluck, F. C. & Kothari, D. S., 1943. The kinetic theory of rubber. *The Journal of Chemical Physics,* 11(8), pp. 387-392.

Baan, R. et al., 2006. Carcinogenicity of carbon black, titanium dioxide, and talc. *The Lancet oncology,* 7(4), p. 295.

Bagrodia, S., Tant, M. R., Wilkes, G. L. & Kennedy, J. P., 1987. Sulphonated polyisobutylene telechelic ionomers: 12. Solid-state mechanical properties. *Polymer,* Volume 28, pp. 2207-2226.

Barbin, W. W. & Rodgers, M. B., 2005. The Science of Rubber Compounding. In: J. E. Mark, B. Erman & F. R. Eirich, eds. *Science and Technology of Rubber, 3rd edition.* Boston: Elsevier Academic Press, pp. 419-469.

Boyd, R. H. & Pant, P. V. K., 1991. Molecular packing and diffusion in polyisobutylene. *Macromolecules,* 24(23), pp. 6325-6331.

Brown, R., 2006. Dynamic Stress and Strain Properties. In: *Physical Testing of Rubebr.* New York: Springer, pp. 173-180.

Chang, J.-H., Uk An, Y. & Soo Sur, G., 2003. Poly(lactic acid) nanocomposites with various organoclays. I. Thermomechanical properties, morphology, and gas permeability. *Journal of Polymer Science Part B: Polymer Physics,* 41(1), pp. 94-103.

Coran, A. Y., 2005. Vulcanization. In: *Science and Technology of Rubber, 3rd edition.* Boston: Elsevier Academic Press, pp. 321-364.

Dluzneski, P. R., 2001. Peroxide Vulcanization of Elastomers. *Rubber Chemistry and Technology,* 74(3), pp. 451-493.

Durán, J. D. G., Ramos-Tejada, M., Arroyo, F. J. & González-Caballero, F., 2000. Rheological and electrokinetic properties of sodium montmorillonite suspensions. *Journal of colloidal and iterface science,* Volume 229, pp. 107-117.

Duvdevani, I. & Frederick-Newman, N., 1997. *Low bromine isobutylene-co-4-bromomethylstyrene compositions for severe duty elastomer applications.* US, Patent No. 5698640.

Eisenberg, A., Farb, H. & Cool, L., 1966. Glass Transition in Ionic Polymers. *Jounral of polymer Science. Part B: Polymer Physics,* 4(6), pp. 855-868.

Eisenberg, A. & Hird, B., 1992. Sizes and Stabilities of Multiplets and Clusters in Carboxylated and Sulfonated Styrene Ionomers. *Macromolecules,* Volume 25, pp. 6466-6474.

Eisenberg, A., Hird, B. & Moore, B., 1990. A new multiplet-cluster model for the morphology of random ionomers. *Macromolecules,* Volume 23, pp. 4098-4107.

Eisenberg, A. & Kim, J.-S., 1998. *Introduction to ionomers.* New York: s.n.

Eisenberg, A., Matsura, H. & Yokoyama, T., 1971. Glass Transition in Ionic Polymers: The Acrylates. *Journal of Polymer Science. Part B: POlymer Physics,* 9(12), pp. 2131-2135.

Eisenberg, A., Matsuura, H. & Yokoyama, T., 1971. The Glass Transition of Aliphatic Ionenes. *Polymer Journal,* Volume 2, pp. 117-123.

Eisenberg, A. & Rinaudo, M., 1990. Polyelectrolytes and ionomers. *Polymer Bulletin,* 24(6), p. 671.

Feldheim, D. L., Lawson, D. R. & Martin, C. R., 1993. Influence of the sulfonate countercation on the thermal stability of Nafion perfluorosulfonate membranes. *Journal of polymer science Part B: polymer physics,* Volume 31, pp. 953-957.

Flory, P. J., 1953. Principle of polymer chemistry. In: *Chap 11.*. New York: Cornell University Press.

Gilman, J. W., Jackson, C. L., Morgan, A. B. & Harris, R., 2000. Flammability Properties of Polymer−Layered-Silicate Nanocomposites. Polypropylene and Polystyrene Nanocomposites. *Chemistry of Materials,* 12(7), pp. 1866-1873.

Gomes-Lage, L., Gomes-Delgado, P. & Kawano, Y., 2004. Vibrational and thermal characterization of Nafion membranes substituted by alkaline earth cations. *European Polymer Journal,* Volume 20, pp. 1309-1316.

Gordon, J. E., 1965. Fused organic salts. III. Chemical stability of molten tetra-n-alkylammonium salts. Medium effects on thermal R4N+X- decomposition. RBr + I- = RI + Br- equilibrium constant in fused salt medium. *Journal of the American Chemical Society,* Volume 87, pp. 2760-2763.

Gorrasi, G. et al., 2003. Vapor barrier properties of polycaprolactone montmorillonite nanocomposites: effect of clay dispersion. *Polymer,* 44(8), pp. 2271-2279.

Heinrich, U. et al., 1994. The Carcinogenic Effects of Carbon Black Particles and Tar–Pitch Condensation Aerosol after Inhalation Exposure of Rats. *The Annals of Occupational Hygiene,* Volume 38, pp. 351-356.

Hirasawa, E., Yamamoto, Y., Tadano, K. & Yano, S., 1991. Effect of the metal cation type on the structure and properties of ethylene ionomes. *Journal of Applied Polymer Science,* Volume 42, pp. 351-362.

Hopkins, W., von Hellens, W., Koski, A. & Rausa, J., 2002. Bromobutyl in Tire Treads. *Rubber World,* Volume 226, pp. 38-43.

Kaszas, G., 2001. *Faster curing, higher torque, stable modulus, improved hot air aging, and improved aged flexure properties; for production of tires.* US, Patent No. 6960632.

Kato, M. et al., 2006. Preparation and properties of isobutylene–isoprene rubber–clay nanocomposites. *Journal of Polymer Science, Part A: Polymer Chemistry,* 44(3), pp. 1182-1188.

Kennedy, J. P. & Marechal, E., 1982. *Carbocationic polymerization.* New York: wiley-Interscience.

Kim, S. et al., 2008. Ionic conductivity of polymeric nanocomposite electrolytes based on poly(ethylene oxide) and organo-clay materials. *Colloids and Surfaces A: Physicochemical and Engineering Aspects,* Volume 313, pp. 216-219.

Kleczek, Monika R. 2013. "Elastomeric ionomers: properties of imidazolium bromide derivatives of poly(isobutylene-co-isoprene)." Kingston, Ontario. Unpublished Manuscript, Queen's University.

Kunal, K. et al., 2008. Polyisobutylene: a most unsual polymer. *Journal of polymer science. Part B: Polymer Physics,* Volume 46, pp. 1390-1399.

Le Bras, J. & Papirer, E., 1979. The Filler—Elastomer Chemical Link and the Reinforcement of Rubber. *Rubber Chemistry and Technology,* 52(1), pp. 43-49.

Lee, J. A., Kontopoulou, M. & Parent, S. J., 2005. Synthesis and characterization of polyethylene-based ionomer nanocomposites. *Polymer,* 46(14), pp. 5040-5049.

Li, Y.-C.et al., 2010. Flame retardant behavior of polyelectrolyte-clay thin film assemblies on cotton fabric. *ACS Nano,* 4(6), pp. 3325-3337.

Loan, L. D., 1964. The reaction between dicumyl peroxide and butyl rubbers. *Jounal of Polymer Science: Part A: Polymer Chemistry,* Volume 2, pp. 2127-2134.

Malmberg, S. M., Parent, J. S., Pratt, D. A. & Whitney, R. A., 2010. Isomerization and elimination reactions of brominated poly(isobutylene-co-isoprene). *Macromolecules,* Volume 43, pp. 8456-8461.

Parent, J. S., Liskova, A. & Resendes, R., 2004. Isobutylene-based ionomer composites: siliceous filler reinforcement. *Polymer,* 45(24), pp. 8091-8096.

Parent, J. S., Liskova, A. & Resendes, R., 2004. Isobutylene-Based Ionomer Composites: Siliceous Filler Reinforcement. *Polymer,* Volume 45, pp. 8091-8096.

Parent, J. S., Malmberg, S., McLean, J. K. & Whitney, R. A., 2010. Nucleophlic catalysis of halide displacement from brominated poly(isobutylene-co-isoprene). *European Polymer Journal,* Volume 46, pp. 702-708.

Parent, J. S., Malmberg, S. M. & Whitney, R. A., 2011. Auto-catalytic chemistry for the solvent-free synthesis of isobutylene-rich ionomers. *Green Chemistry,* Volume 13, pp. 2818-2824.

Parent, J. S. et al., 2004. Synthesis and characterization of isobutylene-based ammonium and phosphonium bromide ionomers. *Macromolecules,* 37(20), pp. 7477-7483.

Parent, J. S., Porter, A. M. J., Kleczek, M. R. & Whitney, R. A., 2011. Imidazolium Bromide Derivatives of poly(isobutylene-co-isoprene): A New Class of Elastomeric Ionomers. *Polymer*, 52(24), pp. 5410-5418.

Parent, J. S. et al., 2003. Sulfuration and reversion reactions of brominated poly(isobutylene-co-isoprene). *Journal of Polymer Science: Part A: Polymer Chemistry*, Volume 41, pp. 1915-1926.

Parent, J. S., White, G. D. F. & Whitney, R. A., 2002. Amine Substitution Reactions of Brominated Poly(isobutylene-co-isoprene): New Chemical Modification and Cure Chemistry. *Macromolecules*, Volume 35, pp. 3374-3379.

Powers, K. W. et al., 1992. *Para-alkylstyrene/isoolefin copolymers and functionalized copolymers thereof.* US, Patent No. 5162445.

Puskas, J. E. & Kaszas, G., 2003. Carbocationic Polymerization. In: *Encyclopedia of polymer science and technology.* s.l.:Wiley-InterScience, pp. 382-418.

Rees, R. W. & Vaughan, D. J., 1965. *Surlyn A Ionomers. The effect of ionic bonding on polymer structure*, s.l.: s.n.

Resendes, R., Krista, R. & Hickey, J. N., 2010. *Butyl ionomer having improved surface adhesion.* USA, Patent No. 7,662,480.

Shaffer, T., Tsou, A. & Webb, R., 2003. Butyl Rubber. In: *Kirk-Othmer Encyclopedia of Chemical Technology.* s.l.:John Wiley and Sons.

Tant, M. R., Wilkes, G. L., Storey, R. & Kennedy, J. P., 1985. Sulfonated Polyisobutylene Telechelic Ionomers. *Polymer Bulletin*, Volume 13, pp. 541-548.

Thomas, D. K., 1961. The Degradation of polyisobutylene by Dicumyl Peroxide. *Transactions of the Faraday Society,* Volume 57, pp. 511-517.

Visser, S. A. & Cooper, S. L., 1991. Comparison of the physical properties of carboxylated and sulfonated ionomers. *Macromolecules,* Volume 24, pp. 2576-2583.

Vukov, R., 1984. *Rubber Chemistry and Technology,* 57(275).

Weiss, R. A., Agarwal, P. K. & Lundberg, R. D., 1984. Control of ionic interactions in sulfonated polystyrene ionomers by the use of alkyl-substituted ammonium counterions. *Journal of applied polymer science,* Volume 29, pp. 2719-2734.

Xiao, S., Parent, J. S., Whitney, R. A. & Knight, L. K., 2010. Synthesis and Characterization of poly(isobutylene-co-isoprene)-derived Macro-monomers. *Journal of Polymer Science Part A: Polymer Chemistry,* Volume 48, pp. 4691-4696.

Xu, Y., Ren, X. & Hanna, M. A., 2006. Chitosan/clay nanocomposite film preparation and characterization. *Journal of Applied Polymer Science,* Volume 99, pp. 1684-1691.

Chapter 2

Design, synthesis and characterization of IIR and IMS-derived functional macro-monomers

2.1. Introduction

Poly(isobutylene-co-isoprene), also known as butyl rubber or IIR, is a random copolymer of isobutylene and 1-2 mol% isoprene with a glass transition temperature of -69ºC. Some of the key features of this polymer and its derivatives are their excellent thermal aging, good damping properties at room temperature, exceptional impermeability to air and moisture due to the close packing of the isobutylene chain segments (Pant & Boyd, 1991), good flexibility at low temperatures due to its low glass transition temperature and good resistance to heat, chemical and oxidative degradation due to the high C-H bond dissociation energy of pendant methyl groups and the steric hindrance that these groups provide towards the backbone chain. However, among its drawbacks are its low strength, little flexibility compared to other polymers and poor adhesion to mineral substrates such as glass or metals.

Polyisobutylene (PIB) does not undergo free radical cross-linking when heated with peroxide initiators, but rather loses molecular weight to macroradical cleavage (Thomas, 1961; Loan, 1964). This feature makes PIB unsuitable for applications requiring dimensional stability under prolonged periods of stress. In the case of IIR, its randomly distributed isoprene mers serve as reactive sites for sulphur cures, making this polymer a good choice for certain applications such as the manufacture of inner tubes. The residual unsaturation within IIR also mitigates radical scission, with isoprene contents greater than 3 mol% giving a copolymer that no longer degrades

(Loan, 1964). Later studies have shown that IIR grades with much higher isoprene contents will cross-link in peroxide formulations containing bismaleimide coagents (Kawachi, et al., 1999). While cure performance improves with increasing isoprene content (Knight, et al., 2010), residual C=C could compromise the long-term aging characteristics of the rubber due to the susceptibility of these groups to oxidation and ozonolysis (Kirk-Othmer, 2004).

The development of halogenated derivatives of butyl rubber in the 1950s helped to overcome some of the disadvantages of butyl rubber, particularly its poor vulcanization reactivity (Franta, 2012) and its incompatibility with diene-rich elastomers such as natural rubber (NR), butadiene rubber (BR) and styrene butadiene rubber (SBR) that are used in tire compounds (Morrissey, 1955). Brominated poly(isobutyl-co-isoprene) rubber (BIIR) contains 1-2 mol% allylic bromide functionality (Chu & Vukov, 1985) and therefore it can undergo a wide range of nucleophlic substitution reactions with amines (Malmberg, et al., 2010) (Parent, et al., 2002), phosphines (Parent, et al., 2004), thiolates (Parent, et al., 2002) and alkoxy nucleophiles (Guillén-Castellanos, et al., 2008), among other functional groups.

Acrylate and vinylbenzoate ester derivatives of BIIR have been shown to cure to a high extend when treated with small amounts of dicumyl peroxide (Xiao, et al., 2010). Additionally, IIR carrying pendant itaconate functionality provides good cure rates while also providing with a potential site for further functionalization. A BHT functionalized itaconate grafted on IIR was shown to stabilize the resulting macro-monomer with respect to radical activity, while retaining the ability to crosslink in the presence of low amounts of peroxide (Shanmugam, 2012). In the same study, a fluorocarbon itaconate grafted IIR macro-monomer proved to display lower surface energy when compared to a hydrocarbon ester IIR macro-monomer, which resulted in smoother flow

characteristics at low shear rate. A schematic representation of the synthesis of these macromonomers is shown in Scheme 2.1.

Scheme 2.1. Synthesis of itaconate diester derivatives of BIIR (Shanmugam, 2012)

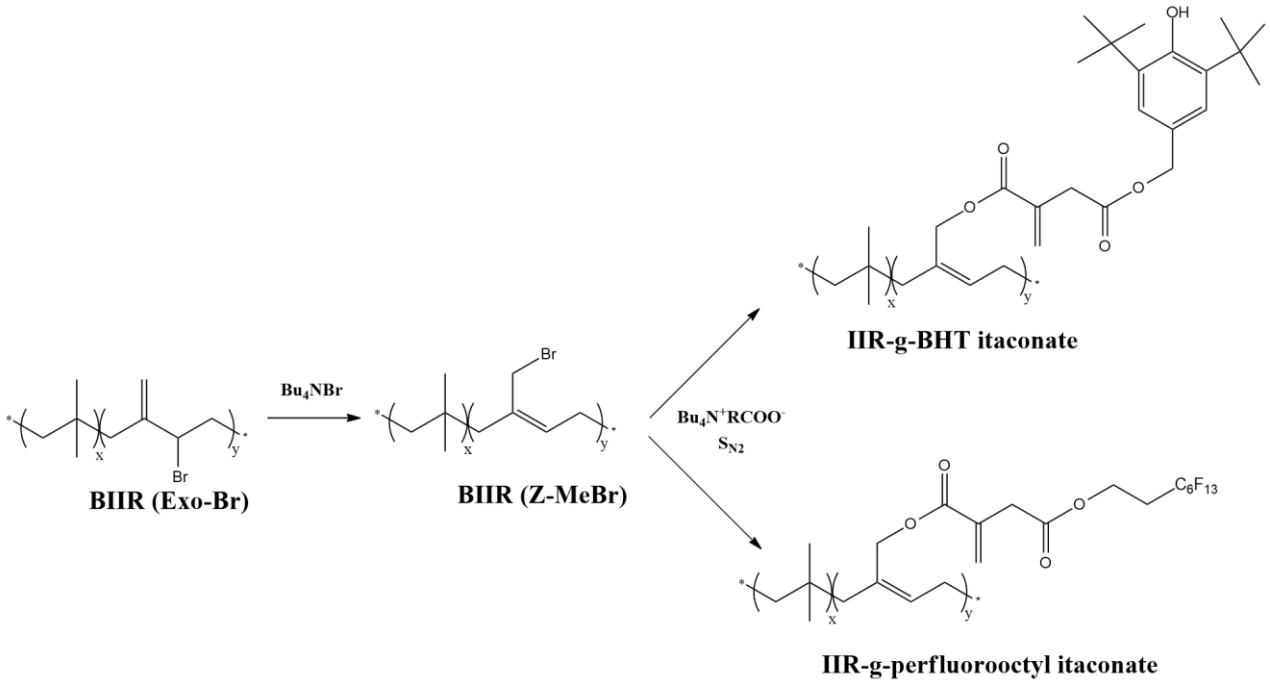

This chapter describes the synthesis of cross-linkable BIIR derivatives via chemical modification of BIIR to give materials that cure efficiently, and bear additional desirable functionality (Scheme 2.2). Specifically, peroxide-curable elastomers containing trialkoxysilane groups that facilitate silica filler dispersion are described, along with a material that contains a polymer-bound dye.

Scheme 2.2. Synthesis of functionalized itaconate grafted macromonomers of IMS and IIR

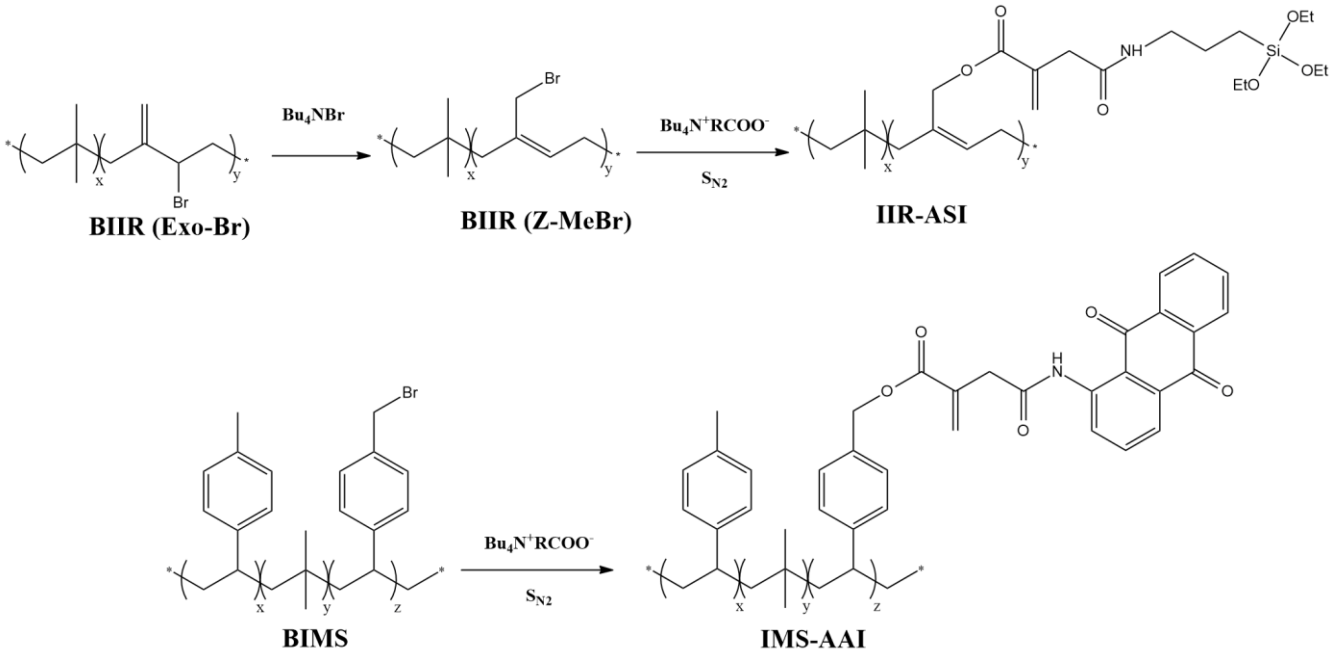

2.2. Experimental

Materials

Itaconic anhydride (95%), 1-dodecanol (95%), tetrabutylammonium bromide (98%), 3-aminopropyltriethoxysilane (99%), tetrabutylammonium hydroxide (1M solution in methanol, 98%), dicumyl peroxide (98%), 1-aminoanthraquinone (97%) were used as received from Sigma-Aldrich. BIIR (LANXESS Bromobutyl 2030, approx. 0.15mmol/gm of allylic bromide) and BIMS (ExxonMobile Exxpro 3745, approx. 0.23 mmol/gm of benzylic bromide) were used as received.

Macro-monomer Synthesis

The multi-functional macro-monomers were prepared by nucleophilic displacement of bromine from BIIR by using the required carboxylate salt. These syntheses involved the pre-isomerization of the exo-allylic bromide functionality within the starting material to E,Z-BrMe isomers by reaction with Bu_4NBr. This was done to generate a more reactive electrophile, thereby increasing esterification rates (Parent, et al., 2010) and limiting the time that potentially sensitive macro-monomer functional groups would be maintained in solution at elevated temperature.

Synthesis of IIR-g-dodecyl itaconate (IIR-DDI)

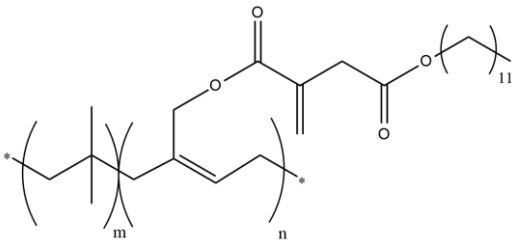

Synthesis of IIR-g-dodecyl itaconate was performed as previously reported by our group (Shanmugam, et al., 2012). The following synthesis were based on this experimental procedure. 1-Dodecanol (8.0mmol,1.5g) and itaconic anhydride (24 mmol, 2.7 g), were dissolved in toluene (10g) and heated to 80°C for 4hr. Residual starting materials and solvent were removed by Kugelrohr distillation (T= 80°C, P=0.6mmHg). The resulting acid-ester was isolated and dried. ^{1}HNMR (DMSO-d_6): δ 6.14 (d, HOOC-C**(=CH_2)**-CH_2-COO-, 1H), δ 5.74 (d, HOOC-C**(=CH_2)**-CH_2-COO-, 1H), δ 3.28 (s, HOOC-C**(**=CH_2**)**-C**H_2**-COO-, 1H) δ 3.98 (t, -CH_2-COO-C**H_2**-, 2H), δ 1.52 (m, -COO-CH_2-C**H_2**-, 2H), δ 1.36 (m, -COO-$(CH_2)_{10}$-C**H_2**-CH_3, 2H), δ 1.25 (m, -CH_2-(C**H_2**)$_9$- CH_2-CH_3, 18H), δ 0.87 (t, CH_2-C**H_3**, 3H). HR MS calculated for $C_{17}H_{31}O_4$ 299.2225; found for $C_{17}H_{31}O_4$: 299.2222.

Monododecyl itaconate (0.98 g, 3.3mmol) was treated with a 1M solution of Bu_4NOH in methanol (3.3ml, 3.3mmol Bu_4NOH) to yield the desired Bu_4Ncarboxylate salt, which was isolated by removing methanol under vacuum. BIIR (11g) and Bu_4NBr (0.53 g, 1.65mmol) were dissolved

in toluene (100g) and heated to 85°C for 180 min. Bu_4Ncarboxylate salt (1.78g, 3.3mmol) was added before heating the reaction mixture to 85°C for 60 min. The esterification product was isolated by precipitation from excess acetone, purified by dissolution/precipitation using hexanes/acetone, and dried under vacuum, yielding IIR-g-dodecyl itaconate. ^{1}H-NMR ($CDCl_3$) : δ 6.24 (s, C**H₂**=C(CH_2)-COO-, 1H), δ 5.62 (s, C**H₂**=C(CH_2)-COO-, 1H), δ 3.36 (s, CH_2=C(C**H₂**)-COO-, 2H), δ 4.54 (E-ester, =CH-**CH₂**-OCO-, 2H, s), δ 4.60 (Z-ester, =CH-**CH₂**-OCO-, 2H, s).

Synthesis of IIR-g-aminopropyltriethoxysilyl itaconate (IIR-ASI)

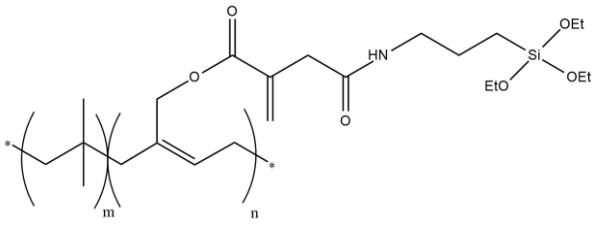

3-aminopropyltriethoxysilane (0.74g, 3.3mmol,) and itaconic anhydride (0.45g, 3.6mmol) were dissolved in THF (15g) and stirred at room temperature for 1 hour. Residual starting materials and solvent were removed by Kugelrohr distillation (T= 80°C, P=0.6mmHg). The resulting acid-amide was isolated. ^{1}HNMR ($CDCl_3$): δ 6.14 (d, HOOC-C**(=CH₂)**-CH_2-CON-, 1H), δ 5.70 (d, HOOC-C**(=CH₂)**-CH_2-CON-, 1H), δ 3.70 (s, HOOC-C(=CH_2)-C**H₂**-CON-, 2H), δ 3.36 (s, HOOC-C(=CH_2)-C**H₂**-CON-, 2H), δ 3.28 (q, -CON-(CH_2)$_3$-Si-(O-C**H₂**-CH_3)$_3$, 6H), δ 3.28 (t, -CON-C**H₂**-(CH_2)$_2$-, 2H), δ 1.79 (m, -CON-CH_2-C**H₂**-CH_2-Si-, 2H), δ 1.58 (t, -CON-(CH_2)$_3$-Si-(O-CH_2-C**H₃**)$_3$, 9H), δ 0.55 (t, -CON-CH_2-CH_2-C**H₂**-Si-, 2H).

3-aminopropyltriethoxysilyl itaconate (1.10 g, 3,3mmol) was treated with a 1M solution of Bu_4NOH (3.3ml, 3.3mmol Bu_4NOH) to yield the desired Bu_4Ncarboxylate salt, which was isolated by removing methanol under vacuum. BIIR (11g) and Bu_4NBr (0.53 g, 1.65mmol) were dissolved in toluene (100g) and heated to 85°C for 180 min. Bu_4Ncarboxylate salt (1,9g, 3.3mmol) was added before heating the reaction mixture to 85°C for 60 min. The esterification product was isolated by precipitation from excess acetone, purified by dissolution/precipitation using

THF/acetone, and dried under vacuum, yielding IIR-g-aminopropyltriethoxysilyl itaconate. ^{1}HNMR ($CDCl_3$): δ 6.35 (d, HOOC-C**(=CH_2)**-CH_2-CON-, 1H), δ 5.72 (d, HOOC-C**(=CH_2)**-CH_2-CON-, 1H), δ 3.34 (q, -CON-$(CH_2)_3$-Si-(O-C**H_2**-$CH_3)_3$, 6H), δ 4.51 (E-ester, =CH-**CH_2**-OCO-, 2H, s), δ 4.67 (Z-ester, =CH-**CH_2**-OCO-, 2H, s).

Synthesis of IMS-g-itaconamido anthraquinone (IMS-AAI)

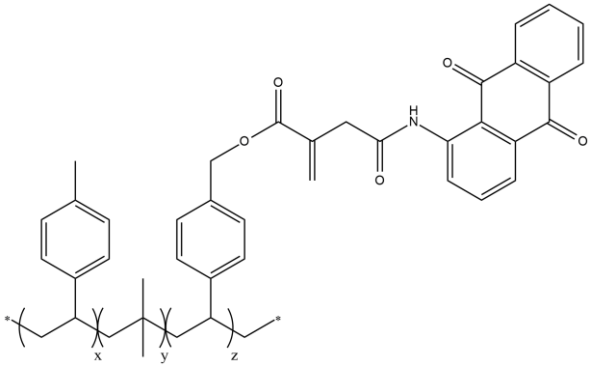

1-Aminoanthraquinone (0.74g, 3.3.mmol) and itaconic anhydride (0.45g, 3.6mmol) were dissolved in toluene (10g) and stirred at 80°C for 2hr. Residual starting materials and solvent were removed by Kugelrohr distillation (T= 80°C, P=0.6mmHg). The resulting acid-amide (AAI) was isolated. ^{1}HNMR ($CDCl_3$): δ 8.32 (m, 8,5-anthraquinone , 2H), δ 8.09 (dd, 2-anthraquinone, 1H), δ 7.80 (d, 7-anthraquinone , 1H), δ 7.70 (d, 6-anthraquinone , 1H), δ 7.52 (t, 3-anthraquinone, 1H), δ 7.02 (dd, 4-anthraquinone, 1H), δ 6.64 (d, HOOC-C**(=CH_2)**-CH_2-CON-, 1H), δ 6.06 (d, HOOC-C**(=CH_2)**-CH_2-CON-, 1H), δ 3.62 (s, HOOC-C(=CH_2)-C**H_2**-CON-, 2H).

1-itaconamido anthraquinone (1.05 g, 3,3mmol) was treated with a 0.5mL of pyridine for 1hr. BIMS (10g) was dissolved in toluene (100g) and the solution of AAI in pyridine was added. The mixture was stirred at 85°C overnight. The esterification product was isolated by precipitation from excess acetone, purified by dissolution/precipitation using THF/acetone, and dried under vacuum, yielding IMS-g-itaconamido anthraquinone (IMS-AAI). ^{1}HNMR ($CDCl_3$): δ 8.32 (m, 8,5-anthraquinone , 2H), δ 8.09 (dd, 2-anthraquinone, 1H), δ 7.80 (d, 7-anthraquinone , 1H), δ 7.70 (d, 6-anthraquinone , 1H), δ 7.52 (t, 3-anthraquinone, 1H), δ 7.02 (dd, 4-anthraquinone, 1H), δ 6.67

(d, -OOC-C**(=CH_2)**-CH_2-CON-, 1H), δ 6.27 (d, HOOC-C**(=CH_2)**-CH_2-CON-, 1H), δ 5.09 (s, ester, 2H), δ 3.77 (s, -OOC-C(=CH_2)-C**H_2**-CON-, 2H), 4.34 (residual BIMS).

Preparation of filled composites

The required amount of product was mixed with 30% wt. silica at 100ºC and 60rpm for 20min using a Haake Polylab R600 internal batch mixer.

Instrumentation and analysis

^{1}H-NMR spectra were acquired in $CDCl_3$ on a Bruker Avance-600 spectrometer. Mass spectra were obtained on an Applied Biosystems QStar XL QqTOF mass spectrometer. Dynamic shear modulus measurements were recorded using an Alpha Technologies, Advanced Polymer Analyzer 2000. Pressed samples of elastomer were coated with the required amount of a stock solution of DCP in acetone, and allowed to dry prior to passing ten times through a 2-roll mill. This mixed compound was cured in the rheometer cavity at 3° oscillation arc and a frequency of 1 Hz at 160°C.

Tensile strength data was acquired using an INSTRON Series 3360 universal testing machine operating at a crosshead speed of 500 mm/min at room temperature. The Young's Modulus was found by calculating the slope of the stress (MPa) between 0 and 0.6 mm strains. Dogbones were cut using a specimen cutter as described in ASTM D4482. Five replicate measurements were made for each sample to test the precision of the compounding and physical testing procedures. UV-vis spectra were obtained using a Cary 100 UV-vis spectrophotometer.

2.3. Results and discussion

A disadvantage of isobutylene-rich elastomers is the susceptibility of the isobutylene backbone chain to undergo degradation. Hydrogen atom abstraction from primary alkyl positions yields macroradicals whose fragmentation results in a loss of molecular weight, and an accompanying reduction of storage modulus (G'). As described above, the grafting of polymerizable functional groups by nucleophilic displacement of bromide from BIIR yields macromonomer derivatives that can crosslink to high extent when heated with standard peroxide initiators. Pendant acrylate and methacrylate groups have received considerable attention, since BIIR can engage carboxylate nucleophiles to give the corresponding esters in quantitative yield. Ring opening of itaconic anhydride with primary alcohols or amines can provide a methacrylate analogue that, depending on the structure of the reagent, can bear additional reactive functionality.

Figure 2.1 provides plots of storage modulus against time for IIR and a macromonomer bearing dodecyl ester functionality (IIRDDI). Each material was mixed with 18.5 μmole of dicumyl peroxide per gram of rubber and heated at 160º in the cavity of a dynamic oscillatory rheometer. Note that determining the chemical structure of thermoset materials is complicated by the insolubility of crosslinked polymers. However, indirect measures of crosslink density can be obtained by monitoring the dynamic storage modulus (G') over the course of the curing process. Changes in molecular weight translate into measurable shifts in G', providing a mean of tracking the competition between macro-monomer crosslinking and polymer backbone degradation. The data presented in Figure 2.1 clearly illustrate the ability of IIRDDI to engage in peroxide curing to give a tightly crosslinked thermoset, while IIR suffers a small extent of degradation under identical reaction conditions.

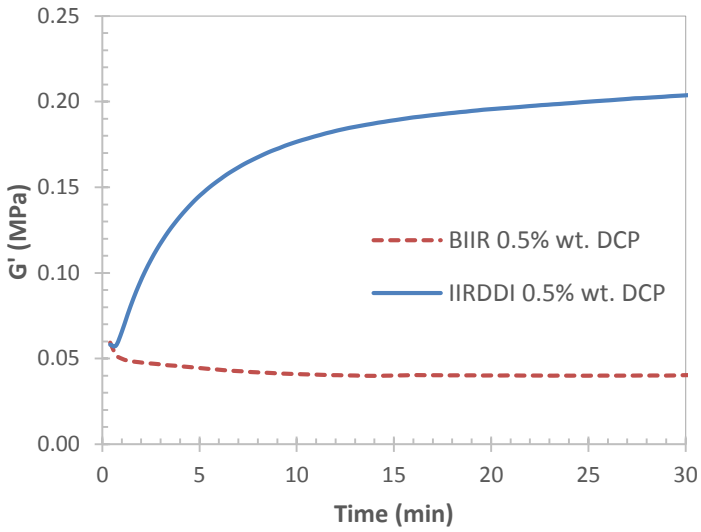

Figure 2.1.Peroxide crosslinking dynamics for IIR and IIR-DDI (160ºC, 1Hz, 3º, 18.5 µmol DCP / g)

The development of new, functional, macromonomers began with studies of 3-aminopropyltriethoxysiloxane. This compound is widely used as a coupling agent in silica-filled composites. Note that silica is commercially used as filler due to its low cost and non-black color, but silanol groups (-Si-OH) on the surface impart a high surface energy, resulting in severe particle aggregation when they are mixed with non-polar elastomers. Silane-coupling agents covalently-bond silica to the elastomer during compound mixing. The trialkoxylsilyl functionality of the silane-coupling agent reacts with the silanol groups of the silica surface, while the amine functionality usually engages in polymer cure chemistry during a sulfur vulcanization process (Sun, et al., 2005). The improved adhesion between polymer and filler enhances silica dispersion and improves thermoset reinforcement.

A comparison of the docecyl functionalized macromonomer, IIR-DDI, and its silane-functionalized analogue, IIR-ASI, was undertaken by compounding each material with 30% wt. silica at 100ºC for 20 min before adding 18.5 μmol DCP/g. The resulting compounds were cured in the rheometer cavity at 160ºC. Data recorded for the IIR-DDI system (Figure 2.2a) showed that silica raised the compound's initial storage modulus by 133% (0.06 to 0.14 MPa), while the thermoset's final storage modulus was improved by 100% (0.20 to 0.40 MPa). Data recorded for the IIR-ASI system showed higher storage modulus gains (Figure 2.2b). In this case, the initial modulus of the filled compound was 300% greater than the unfilled polymer (0.07 to 0.28 MPa), while the cured thermoset had a storage modulus 282% higher (0.11 to 0.42 MPa).

As expected, the degree of silica filler reinforcement was considerably greater for the aminosilyl itaconate modified rubber. However, the data also indicate that the amide functionality reduced the ultimate cure yield. That is, the difference between the final and initial storage modulus of unfilled IIR-ASI ($\Delta G' = 0.04$ MPa), which is good proxy for crosslink density, was less than that for IIR-DDI ($\Delta G' = 0.17$ MPa). This lower macromonomer crosslinking yield is consistent with literature reports of lower oligomerization rates for N-substituted itaconic esters in free radical polymerization (Watanabe, et al., 1994). In the present context, a lower C=C oligomerization rate makes macromonomer crosslinking less competitive with polymer backbone degradation, resulting in a lower ultimate state of cure.

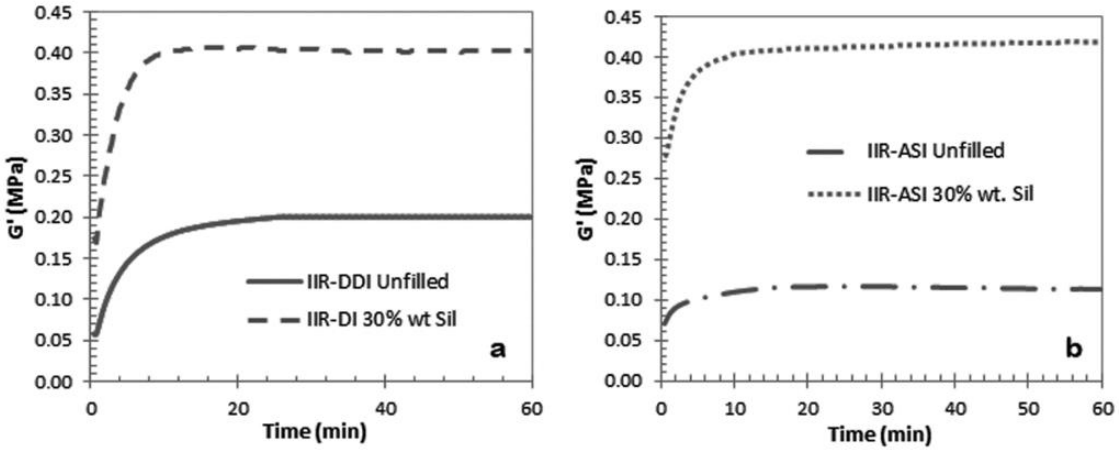

Figure 2.2. Peroxide crosslinking dynamics for silica-filled and gum rubber compounds of (a) IIR-DDI and (b) IIR-ASI (160ºC, 1Hz, 3º, 18.5 µmol DCP/g).

While the cure rheology data presented in Figure 2.2 are useful for probing crosslinking dynamics, a better means of assessing silica dispersion is a Payne analysis, wherein the composite is subjected to an oscillatory shear deformation at an ever-increasing strain amplitude. Composites with poor filler dispersion typically show very high storage moduli at low strain, since material properties in this regime can be dictated by filler particle aggregation. However, these filler-filler interactions act over small distance scales, so composites with poor dispersion soften significantly as the strain amplitude increases to the point where particle contact is broken. In contrast, well-dispersed composites typically have relatively low modulus values at small strains, but maintain this value over a wider range of strain amplitude (Payne & Whittaker, 1971).

Figure 2.3 provides Payne analysis data for both of the 30% wt. silica composites. Note that IIR-DDI displayed a high low-strain modulus that was quite amplitude sensitive, while IIR-ASI exhibited behavior that is consistent with a well dispersed composite. This indicates that the control sample (IIR-DDI) suffers from a strong reticulate network formation at a 30% silica

loading, and the aminosilyl itaconate analogue (IIR-ASI) benefits from improved polymer-filler interactions during the compound mixing process, thereby affording better material properties.

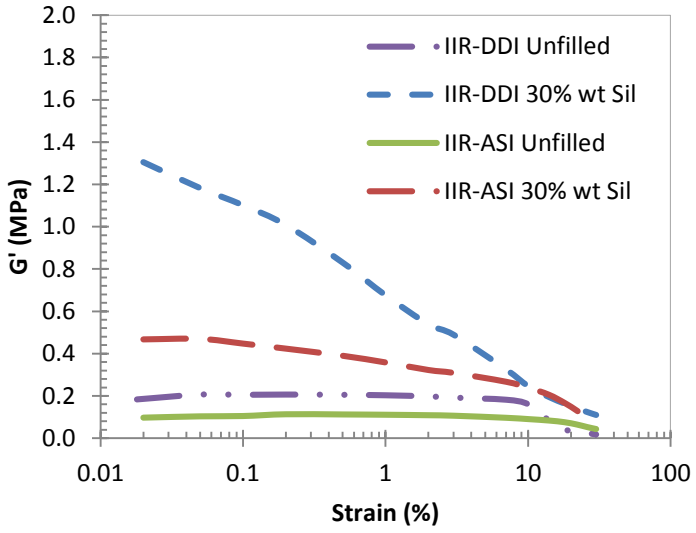

Figure 2.3.Payne analysis for silica-filled IIR-DDI and IIR-ASI (100°C, 0.1Hz)

Static tensile data for the composites are consistent with this conclusion. Figure 2.4 plots stress-strain data that shows the IIR-DDI composite to be very stiff at low elongation, which is a product of silica particle agglomeration. Furthermore, the IIR-DDI control was less stiff at higher elongations, where agglomerates are broken and silica must reinforce the thermoset through strong polymer-filler interactions. The tensile data summary listed in Table 2.1 provides numerical values to support these arguments.

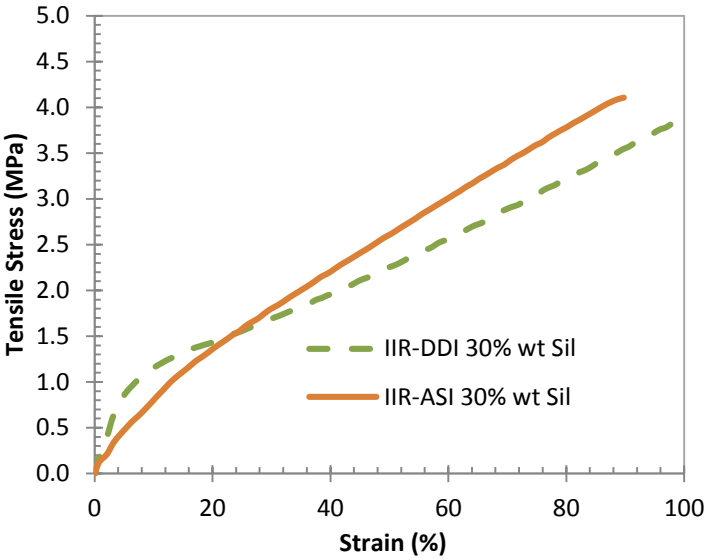

Figure 2.4. Static tensile results for the silica-filled 0.5% wt DCP cured silica-filled IIR-DDI and IIR-ASI samples

Table 2.1. Static tensile data for IIR-DDI and IIR-ASI silica composites

Sample	Young's Modulus (MPa)	Tensile stress at break (MPa)	Tensile strain at break (%)	σ_{100} (MPa)
IIR-DDI 30% wt. Sil	24.2 ± 3.0	3.83 ± 0.20	335 ± 22	3.85 ± 0.11
IIR-ASI 30% wt. Sil	15.5 ± 1.0	13.9 ± 0.8	95 ± 4	4.03 ± 0.23

Many of the synthetic dyes used in textile applications are anthraquinone-based, due to the chemical stability and versatility of this molecule. When mixed into a standard elastomer compound, no covalent bonds exist between polymer and dye, and leaching from the thermoset can result in a loss of color intensity and potential environmental issues. Therefore, the itaconate ester approach was extended to include a polymer-bound chromophore that was introduced to a

macromomomer by the esterification of BIMS. Ring opening of itaconic anhydride with 1-aminoanthraquinone produced the desired amidic acid in good yield, which was subsequently reacted with BIMS under basic conditions to produce the corresponding macromonomer. Figure 2.5 provides UV-vis absorption spectra for the two starting materials, BIMS and 1-aminoanthraquinone, as well as the intermediate amidic acid (AAI), and the macromonomer product, IMS-AAI. 1-aminoanthraquinone is dark red (Egerton & Roach, 1958), and both, the itaconic amide of the dye (AAI), and the polymer-bound itaconamido antrhaquinone (IMS-AAI), were similarly coloured, with maximum absorption wavelengths that varied slightly between the free primary amine its amide derivatives.

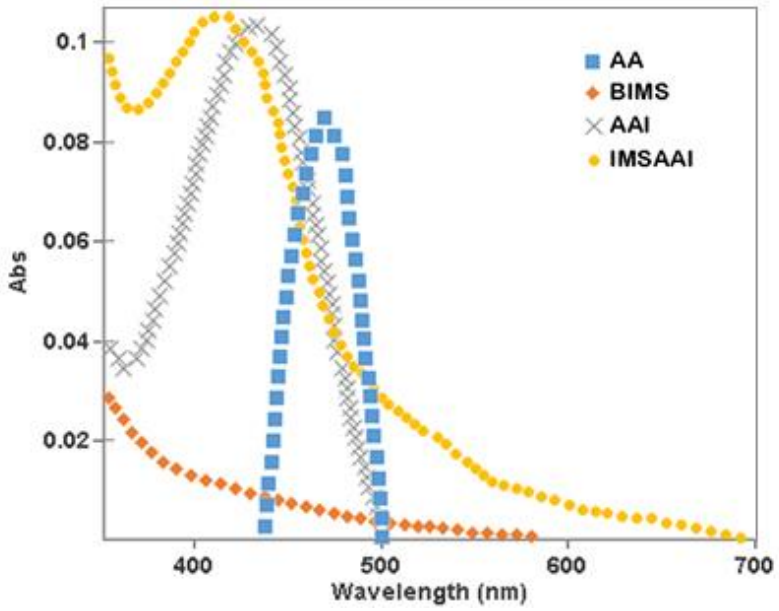

Figure 2.5. UV-vis spectra of 1-aminoanthraquinone (AA), 1-aminoanthraquinoyl itaconate (AAI), BIMS and IMS-AAI.

The introduction of the itaconamido anthraquinone functionality on BIMS to give IMS-AAI reduced the cure yield relative to the alkyl itaconate control sample, IMS-DDI (Figure 2.6). As describe above, this arises because of the lower oligomerization rates reported for N-substituted itaconic esters (Watanabe, et al., 1994). Additionally, 1-aminoanthraquinone has shown polymerization inhibitory effects when compared to other quinone molecules (Georgieff, 1965). However, a product containing just 10% itaconamido anthraquinone and 90% dodecyl itaconate functionality provided cure yields similar to that of IMS-DI, while still exhibiting a strong color.

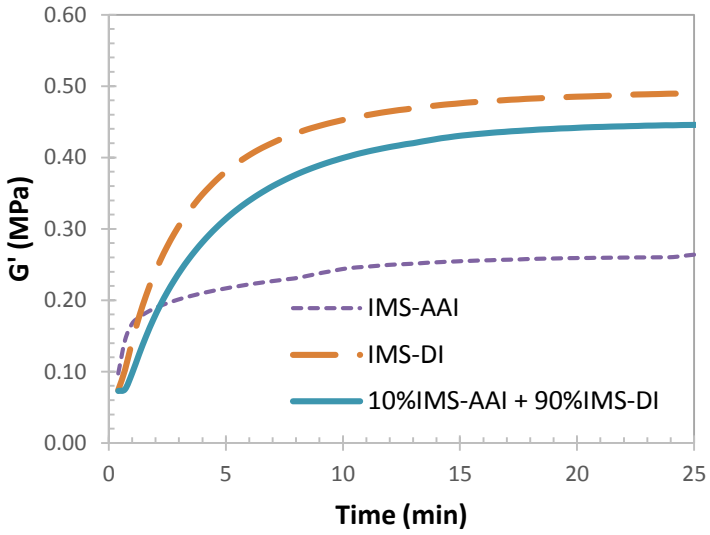

Figure 2.6. Dynamics of peroxide-initiated macro-monomer cross-linking for IMS-AAI, IMS-DI and the mixed product of them ([DCP]= 18µmol/g)

2.4. Conclusions

Ring opening of itaconic anhydride by primary alcohols and amines yields corresponding itaconic half acids that can be used as a nucleophile to chemically modify BIMS. Depending on the structure of the alcohol/amine, the resulting macromonomer can contain polymer-bound

functionality that affects the material's performance. The introduction of aminoalkylsiloxane groups improved the dispersion of silica during rubber compounding, giving a thermoset composite with superior mechanical properties. The incorporation of anthraquinone functionality gave a chromophoric polymer derivative that peroxide-cured to give a coloured material containing polymer-bound dye.

2.5. Works Cited

Chu, C. Y. & Vukov, R., 1985. Determination of the Structure of Butyl Rubber by NMR Spectroscopy. *Macromolecules*, Volume 18, pp. 1423-1430.

Egerton, G. S. & Roach, A. G., 1958. Studies on Aminoanthraquinone Compounds I—Absorption Spectra in Solution and in the Solid State. *Journal of the Society of Dyers and Colourists,* Issue 5, pp. 401-407.

Franta, I., 2012. Elastomers and Rubber Compounding Materials. In: s.l.:Elsevier, pp. 178-180.

Georgieff, K. K., 1965. Relative Inhibitory Effect of Various Compounds on the Rate of Polymerization of Methyl Methacrylate. *Journal of Applied Polymer Science,* Volume 9, pp. 2009-2018.

Guillén-Castellanos, S. A., Parent, J. S. & Whitney, R. A., 2008. Synthesis and Characterization of Ether Derivatives of Brominated Poly(isobutylene-co-isoprene). *Journal of Polymer Science. Part A: Polymer Chemistry,* Volume 44, pp. 983-992.

Kawachi, E., Kawachi, Y., Muraki, T. & Sudo, M., 1999. U.S., Patent No. 5994465.

Kirk-Othmer, 2004. Butyl Rubber. In: *Kirk-Othmer Encyclopedia of Chemical Technology*. 5th ed. s.l.:John Wiley & Sons, Inc..

Knight, L., Ferrari, L., Crockett, T. & Chadder, S., 2010. *Novel Peroxide Curable Butyl Rubber with Fillers,* Milwaukee, WI, United States: American Chemical Society, Rubber Division, 178 Technical Meeting.

Loan, L., 1964. The reaction between dicumyl peroxide and butyl rubbers. *Journal of Polymer Science A: Polymer Chemistry,* pp. 2127-2134.

Malmberg, S. M., Parent, S. J., Pratt, D. A. & Whitney, R. A., 2010. Isomerization and elimination reactions of brominated poly(isobutylene-co-isoprene). *Macromolecules,* pp. 8456-8461.

Morrissey, R., 1955. *Butyl-Type Polymers Containing Bromine.* Brecksville, Ohio, The B. F. Goodrich Company Research Center.

Pant, P. K. & Boyd, R. H., 1991. Molecular packing and diffusion in polyisobutylene. *Macromolecules,* pp. 6325-6331.

Parent, J. S., Malmberg, S., McLean, J. K. & Whitney, R. A., 2010. Nucleophilic catalysys of halide displacement from brominated poly(isobutylene-co-isoprene). *European Polymer Journal,* pp. 702-708.

Parent, J. S. et al., 2004. Synthesis and Characterization of Isobutylene-Based Ammonium and Phosphonium Bromide Ionomers. *Macromolecules,* Volume 37, pp. 7477-7483.

Parent, J. S., White, G. D. & Whitney, R. A., 2002. Amine Substitution Reactions of Brominated Poly(isobutylene-co-isoprene): New Chemical Modification and Cure Chemistry. *Macromolecules,* Volume 35, pp. 3374-4479.

Parent, J. S., White, G. D. & Whitney, R. A., 2002. Synthesis of thioether derivatives of brominated poly(isobutylene-co-isoprene): Direct coupling chemistry for silica reinforcement. *Journal of Polymer Science. Part A: Polymer Chemistry,* Volume 40, pp. 2937-2944.

Payne, A. R. & Whittaker, R. E., 1971. Low Strain Dynamic Properties of Filled Rubbers. *Rubber Chemistry and Technology,* 44(2), pp. 440-478.

Shanmugam, K. V. S., 2012. Design, synthesis and characterization of IIR-derived functional macromonomers. *Unpublished manuscript.*

Shanmugam, K. V. S., Parent, J. S. & Whitney, R. A., 2012. Design, Synthesis and Characterization of Bismaleimide Co-Curing Elastomers. *Industrial & Engineering Chemistry Research,* Volume 51, pp. 8957-8965.

Sun, Y., Zhang, Z. & Wong, C., 2005. Study on mono-dispersed nano-size silica by surface modification for underfill applications. *Journal of Colloid and Interface Science*, 292(2), pp. 436-444.

Thomas, D., 1961. The degradation of polyisobutylene by dicumyl peroxide. *Trans. Faraday Soc.*, pp. 511-517.

Watanabe, H., Matsumoto, A. & Otsu, T., 1994. Radical Polymerization of N-substituted Itaconamic Esters and Itaconamides. *Journal of Polymer Science Part A: Polymer Chemistry*, 32(11), pp. 2085-2091.

Xiao, S., Parent, J. S., Whitney, R. A. & Knight, L. K., 2010. Synthesis and Characterization of Poly(isobutylene-co-isoprene) Derived Macro-Monomers. *Journal of Polymer Science. Part A: Polymer Chemistry*, Volume 48, pp. 4691-4696.

Chapter 3

Effect of counter anions on the properties of imidazolium ionomer derivatives of poly(isobutylene-co-para-methylstyrene)

3.1. Introduction

Brominated poly(isobutylene-co-p-methylstyrene) (BIMS) is an analogue of brominated butyl rubber (BIIR) that contains 0.23mmol/g of benzylic bromide functionality and 0.51mmol/g of unbrominated para-methylstyrene mers, as indicated by the supplier. It provides the low gas permeability that is characteristic of isobutylene-rich elastomers, but is similarly incapable of peroxide-initiated crosslinking. However, the benzylic halide functionality provides the opportunity to introduce peroxide-curable functionality via nucleophilic displacement of bromide. Examples of relevant BIMS derivatives include acrylate esters (Wang, et al., 1994), phosphonium salts (Arjunan, et al., 1998) ammonium salts (Tsou, et al., 2004) and imidazolium salts bearing a range of alkyl and olefinic groups (Ozvald, 2012).

As discussed in the Introduction section, peroxide-cured elastomeric ionomers exhibit material properties that are affected by a covalent cross-link network and an ionic network of associated ion pairs. This hybrid character results in stress relaxation behaviour, temperature sensitivity, and tensile properties that differ substantially from those of conventional covalent thermosets (Parent, et al., 2002). The 1-vinyl-3-alkyl-imidazolium (Scheme 3.1) ionomer derived from BIMS is particularly promising, since it provides high covalent crosslink densities as well as significant ion pair concentrations. However, only the bromide salt has been studied to date. This chapter describes the synthesis and properties of imidazolium derivatives of BIMS bearing different counter anions (bromide, dodecyl sulfate, 4-styrene sulfonate, and montmorillonite clay).

Comparative studies between these ionomers provide insight into the impact of the anion structure on key material properties.

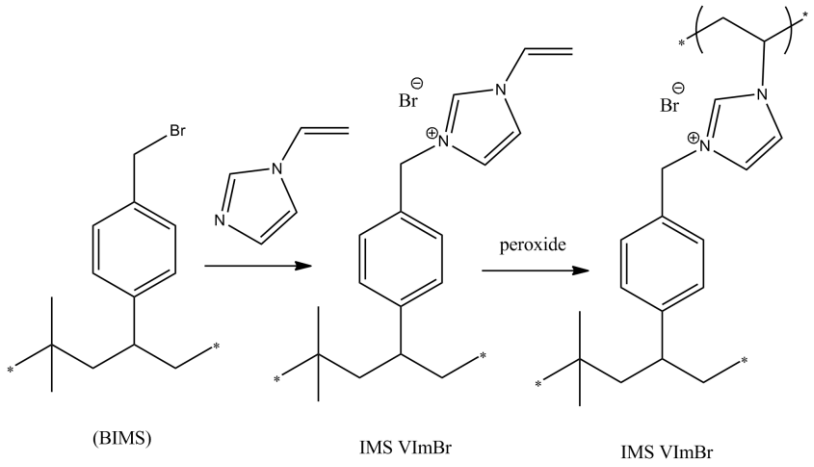

Scheme 3.1. Synthesis and crosslinking reaction of IMS VImBr

3.2. Experimental

Materials

1-Butylimidazole (BuIm, 98%), 1-vinylimidazole (VIm, 99+%), chloroform-*d* (99.8%D), dicumyl peroxide (DCP, 98%), 1M solution of tetrabutylammonium hydroxide in methanol (Bu_4NOH), sodium dodecyl sulfate (98%), sodium styrene sulfonate (98%), dodecanol (98%), and itaconic anhydride (95%) were used as received from Sigma-Aldrich (Oakville, Ontario). Brominated poly(isobutylene-*co*-para-methylstyrene) (BIMS) (Exxpro 3745, 0.23 mmol benzylic bromide functionality/g BIMS) was used as supplied by Exxon Mobil Chemical (Baytown, Texas). Sodium Cloisite was used as supplied by Southern Clay Products Inc. (Gonzales, Texas).

Synthesis of IMSVIm-bromide (IMSVImBr)

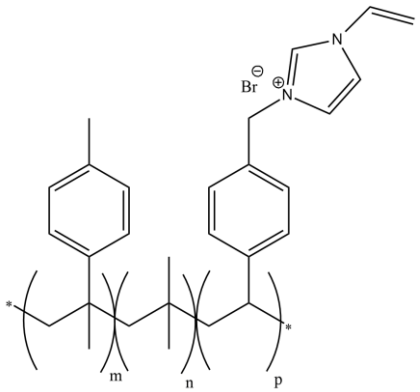

BIMS (40.0 g, 9.2 mmol of benzylic bromide) was mixed with 1-vinylimidazole (1.73 g, 18.4 mmol, 2.0 eq.) at 90ºC and 30 rpm using a Haake Polylab R600 internal batch mixer for 30 min. The final product was characterized by ^{1}H NMR.

^{1}H NMR ($CDCl_3$): δ 10.35(s, 1H, -N^+=C**H**-N-), δ 5.85 (dd, 1H, -N-CH=CH-$\mathbf{H}_{trans}$), δ 5.48 (s, 2H, -Ph-C$\mathbf{H_2}$-N^+-), δ 5.41 (dd, 1H, -N-CH=CH-$\mathbf{H}_{cis}$), δ 5.32 and 4.94 (residual VIm), δ 4.49 (s, 2H, residual BIMS), δ 4.45 (s, 2H, residual BIMS).

Synthesis of IMSBuIm-bromide (IMSBuImBr)

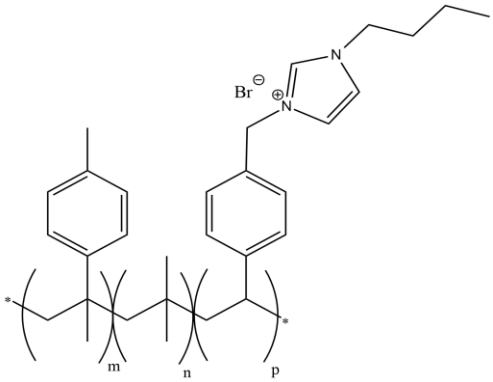

BIMS (40.0 g, 9.2 mmol of benzylic bromide) was mixed with 1-BuIm (1.71 g, 13.8 mmol, 1.5 eq.) at 120ºC and 30 rpm using a Haake Polylab R600 internal batch mixer for 45 min. The final product was characterized by ^{1}H NMR.

^{1}H NMR ($CDCl_3$): δ 9.88 (s, 1H, -N^+=C**H**-N-), δ 5.51 (s, 2H, -C-C$\mathbf{H_2}$-N^+), δ 4.27 (t, 2H, -N-C$\mathbf{H_2}$-CH_2-CH_2 -CH_3), δ 3.91 (residual BuIm), δ 4.49 (s, 2H, residual BIMS), δ 4.45 (s, 2H, residual BIMS).

IMSBuImBr displayed a glass transition temperature of -21ºC, similar to that of BIMS reported in literature (Kumar, et al., 2008).

Synthesis of IMSVIm-dodecylsulfate (IMSVImDS)

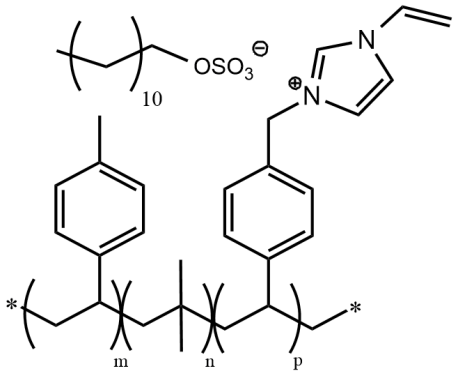

IMSVImBr (40g, 9.2mmol of bromide) was dissolved in 600 ml of toluene and 50 ml of water with sodium dodecyl sulfate (1.03 g, 11 mmol, 1.2 eq.) were added to the solution, the mix was stirred until emulsion appeared and it was left to react for 16hrs. After that, the polymer was precipitated in acetone, purified in THF/acetone and dried under vacuum overnight. The final product was characterized by ^{1}H NMR.

^{1}H NMR ($CDCl_3$): **IMS VIm** δ 10.35(s, 1H, -N^+=C**H**-N-), δ 5.85 (dd, 1H, -N-CH=CH-**H_{trans}**), δ 5.48 (s, 2H, -Ph-C**H_2**-N^+-), δ 5.41 (dd, 1H, -N-CH=CH-**H_{cis}**), **DS** δ 3.96 (t, 2H, -C**H_2**-OSO_3^-), δ 1.60 (q, 2H, CH_3-C**H_2**-), δ 1.21 (m, 18H, CH_3-CH_2-(C**H_2**)$_9$-), δ 0.85 (t, 3H, C**H_3**-CH_2-).

Synthesis of IMSVIm-styrene sulfonate (IMSVImSS)

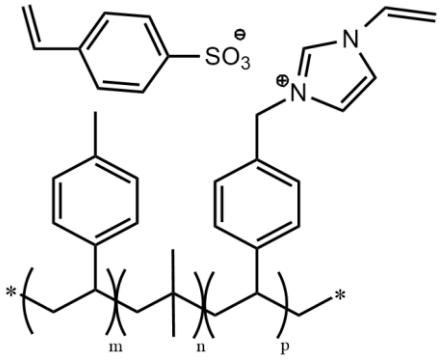

IMS VIm Br (40 g, 9.2 mmol of bromide) was dissolved in toluene (600 mL) and mixed with 50 mL of water with sodium 4-styrenesulfonate (12.4 mmol, 2.6 g), the reaction mixture was stirred for 24 hr. The resulting polymer was isolated by precipitation from excess acetone, purified by dissolution/precipitation using THF/acetone, and dried under vacuum, yielding IMS VIm 4-styrenesulfonate.

^{1}H NMR ($CDCl_3$): **IMS VIm** δ 10.35(s, 1H, -N^+=C**H**-N-), δ 5.85 (dd, 1H, -N-CH=CH-**H_{trans}**), δ 5.48 (s, 2H, -Ph-C**H_2**-N^+-), δ 5.41 (dd, 1H, -N-CH=CH-**H_{cis}**). **SS** δ 6.72 (dd, 1H, Ph-C**H**=CH_2), δ 5.80 (d, 1H, -CH=C**H_{2trans}**), δ 5.30 (d, 1H, -CH=C**H_{2cis}**).

Synthesis of IMSBuIm-dodecyl sulfate (IMSBuImDS)

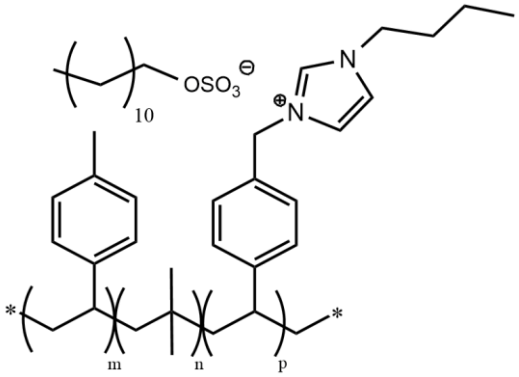

IMSBuImBr (40g, 9.2mmol of bromide) was dissolved in 150ml of toluene and 25ml of water with sodium dodecyl sulfate (3.98.03 g, 13.8 mmol, 1.5 eq.), the mix was stirred and when emulsion appeared it was left to react for 16hrs. After that, the polymer was precipitated in acetone, purified in THF/acetone and dried under vacuum overnight. The final product was characterized by ^{1}H NMR.

^{1}H NMR ($CDCl_3$): **IMSBuIm:** δ 9.88 (s, 1H, -N^+=C**H**-N-), δ 5.51 (s, 2H, -C-C**H_2**-N^+), δ 4.27 (t, 2H, -N-C**H_2**-CH_2-CH_2 -CH_3). **DS** δ 3.96 (t, 2H, -C**H_2**-OSO_3^-), δ 1.60 (q, 2H, CH_3-C**H_2**-), δ 1.21 (m, 18H, CH_3-CH_2-(C**H_2**)$_9$-), δ 0.85 (t, 3H, C**H_3**-CH_2-).

IMSBuImDS displayed a glass transition temperature of -22ºC, similar to that of BIMS reported in literature (Kumar, et al., 2008).

Synthesis of IMSVIm-styrene sulfonate (IMSBuImSS)

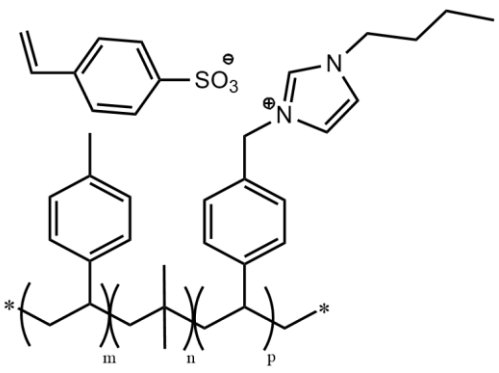

IMSBuImBr (40 g, 9.2 mmol of bromide) was dissolved in toluene (600 mL) and mixed with 50 mL of water with sodium 4-styrenesulfonate (12.4 mmol, 2.6 g), the reaction mixture was stirred for 24 hr. The resulting polymer was isolated by precipitation from excess acetone, purified by dissolution/precipitation using THF/acetone, and dried under vacuum, yielding IMS VIm 4-styrenesulfonate.

^{1}H NMR ($CDCl_3$): **IMSBuIm:** δ 9.88 (s, 1H, -N^+=C**H**-N-), δ 5.51 (s, 2H, -C-C**H_2**-N^+), δ 4.27 (t, 2H, -N-C**H_2**-CH_2-CH_2 -CH_3).**SS** δ 6.72 (dd, 1H, Ph-C**H**=CH_2), δ 5.80 (d, 1H, -CH=C**H_{2trans}**), δ 5.30 (d, 1H, -CH=C**H_{2cis}**).

Synthesis of IMS-dodecyl itaconate (IMS-DI)

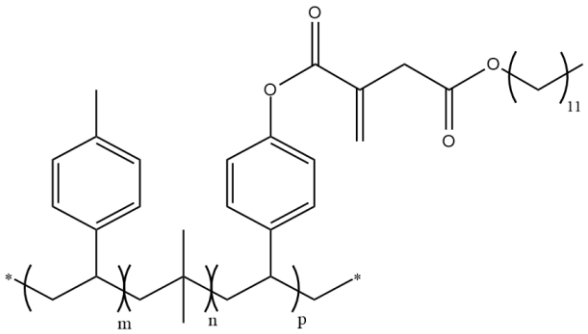

1-Dodecanol (13.8 mmol, 2.6 g) and itaconic anhydride (13.8 mmol, 1.6 g) were mixed and heated to 115°C for 6 hrs. Residual starting materials were removed by Kugelrohr distillation (T= 80°C, P=0.6 mmHg). ^{1}HNMR ($DMSO-d_6$): δ 6.14 (d, HOOC-C**(**=C**H_2)**-CH_2-COO-, 1H), δ 5.74 (d, HOOC-C**(**=C**H_2)**-CH_2-COO-, 1H), δ 3.28 (s, HOOC-C**(**=CH_2)-C**H_2**-COO-, 1H) δ 3.98 (t, -CH_2-COO-C**H_2**-, 2H), δ 1.52 (m, -COO-CH_2-C**H_2**-, 2H), δ 1.36 (m, -COO-$(CH_2)_{10}$-C**H_2**-CH_3, 2H), δ 1.25 (m, -CH_2-(C**H_2**)$_9$- CH_2-CH_3, 18H), δ 0.87 (t, CH_2-C**H_3**, 3H).

The resulting acid-ester (12.4 mmol, 3.7 g) was treated with a 1 M solution of Bu_4NOH in methanol (12.4 mL, 12.4 mmol Bu_4NOH) to yield the desired Bu_4Ncarboxylate salt, which was isolated by removing methanol under vacuum. BIMS (40 g, 9.2 mmol of benzylic bromide) was dissolved in toluene (600 mL) and mixed with Bu_4NDI (12.4 mmol, 6.7 g), the reaction mixture was stirred for 24 hr. The esterification product was isolated by precipitation from excess acetone, purified by dissolution/precipitation using THF/acetone, and dried under vacuum, yielding IMS-dodecyl itaconate.

Synthesis of the mixed alkylated bromide ionomer (IMSMImBr)

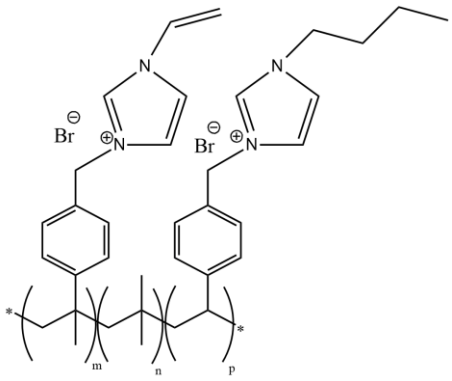

Since BuIm has been found to alkylate faster than VIm (Porter 2011), the alkylation of BuIm was carried out first. BIMS (40g, 9.2 mmol benzylic bromide) was mixed with BuIm (0.64g, 5mmol) at 110°C and 60rpm using a Haake Polylab Mixer R600 Internal batch mixer for 40 mins. After that, the temperature of the mixer was set to 90°C, VIm (0.6g, 6.7mmol) was added and the polymer was mixed for 40 min. The resulting BIMS derivative contained 50% N-vinylimidazolium bromide and 50% N-butylimidazolium bromide functionality. This product was characterized by ^{1}HNMR.

Preparation of Cured Macrosheets

For the case of the vinyl imidazolium salts, a 35.0 g batch of dried elastomer was coated with a solution of 0.175 g of DCP (18.5 μmol DCP/g rubber) in acetone and allowed to dry before being passed through a two-roll mill ten times. The product was then compression molded at 160ºC and 20 MPA for 25 min ($5t_{1/2}$ for DCP). The sheeted products had a thickness of 2.00 ± 0.05 mm. For the case of the butyl imidazolium salts, the same procedure was followed with the exception of the addition of DCP. For the 180º peel tests, the rubber was compressed molded and cured with a Darktek Nylon Film (Alpha Technologies) on top of it.

Preparation of polymer-clay nanocomposites

The required amount of sodium montmorillonite was dispersed in 25mL of DMSO for 1hr and the resulting slurry was added to the polymer solution. The polymer-clay mixture was stirred for 2hrs and then, 10mL of water were added and the two-phase system was stirred until emulsion appeared in order to promote ion metathesis. The polymer was precipitated with acetone, purified

in THF/acetone and dried under vacuum. Once the intercalation was determined by XRD, the nanocomposite was passed 20 times through a heated two-roll-mill at 80ºC.

Instrumentation and analysis

NMR characterization was performed on a BrukerAM400 instrument using deuterated chloroform ($CDCl_3$) as a solvent and with chemical shifts (δ) reported relative to tetramethylsilane in ppm. Rheological characterization was carried out in an oscillatory rheometer (Advanced Polymer Analyzer 2000, Alpha Technologies) operating in parallel plate configuration. For the case of the vinyl imidazolium salts, a 5.0 g sample of the uncured material was coated with the required amount of a solution of DCP in acetone and allowed to dry before being passed through a two-roll mill ten times in order to homogenize the sample. The mixed compound was cured in the rheometer cavity at 160ºC for 60 minutes, at a 3º oscillation arc and a frequency of 1 Hz. Stress relaxation measurements were conducted at 100ºC with a strain of 2º for 5 min. Temperature sweeps were conducted from 100 to 200ºC for the vinyimidazolium ionomers and 40 to 200ºC for the butylimidazolium ionomers at a frequency of 1 Hz and a 3º oscillation arc. Strain sweeps were conducted at 100ºC and a frequency of 0.1Hz. Frequency sweeps were conducted at 100ºC and a 1º oscillation arc.

Tensile strength data were acquired using an INSTRON Series 3369 universal testing instrument, operating at crosshead speed of 500 mm/min at 23 ± 1 ºC. Young's Modulus was found by calculating the slope of the stress (MPa) vs. strain (mm/mm) curve from 0 mm to 0.6 mm of extension. Dogbones were cut from the specimen cutter described in ASTM D4482. Five replicate measurements were made for each sample, and error estimates are reported as +/- one standard deviation. Adhesive strength data were acquired using an INSTRON Series 3369 universal testing

instrument, operating at crosshead speed of 100 mm/min at room temperature. 180º peel tests were performed according to ASTM D413 using nylon sheets as the adhered surface.

X-ray diffraction (XRD) was used to determine the extent of clay exfoliation. A Philips X'Pert Pro Diffractometer (Cu radiation λ = 1.540Å, generator voltage = 45kV, current = 40 μ) operating at a 2Θ range of 3 to 40º and a rate of 1º/min was used. Differential scanning calorimetry (DSC) experiments were performed using a TA-Instruments DSC Q100 modulated differential scanning calorimeter. Samples were kept at 110 ºC for 16 hrs to erase any possible prior thermal history.

Samples for TEM analysis were compression molded and cryosectioned at -90°C and cut in 90nm thickness sections on a Leica Ultracut UCT equipped with a Leica EMFCS cryo-system. The sections were placed on 400 mesh copper grids coated with a carbon film and viewed on a FEI Tecnai 20 TEM operated at 200kV. Images were captured on an AMT 16000 camera.

3.3. Results and discussion

Studies of carboxylate and sulfonate ionomers have shown that counter ion size has a significant effect on the physical properties of thermoplastic materials (Weiss, et al., 1984; Hirasawa, et al., 1991; Feldheim, et al., 1993). With the aim of improving knowledge of counter anion effects on elastomeric ionomers, two series of imidazolium bromide derivatives of BIMS were prepared (Parent, et al., 2011). The vinylimidazolium ionomers are capable of peroxide curing to produce a hybrid ionic/covalent network, while the butylimidazolium analogues are not crosslinked by peroxide formulations, but remain thermoformable. ^{1}H NMR confirmation of the imidazolium bromide ionomers was followed by anion metathesis using an emulsion process that facilitates anion exchange by dissolving liberated NaBr in an aqueous phase. The extent of anion

metathesis was assessed by ^{1}H NMR. The addition of two drops of a 5% solution of $AgNO_3$ to the water phase obtained after the precipitation of the polymer caused the appearance of a yellow precipitate of silver bromide that was insoluble in water but soluble in concentrate ammonia. The presence of this precipitate was used to qualitatively confirm the displacement of bromide anion.

Two organic counter anions were examined; one with a long alkyl chain, dodecyl sulfate, and one containing a polymerizable group, styrene sulfonate. A schematic of the ionomers synthesized is shown in Scheme 3.2.

Scheme 3.2. Imidazolium ionomers analyzed in this report

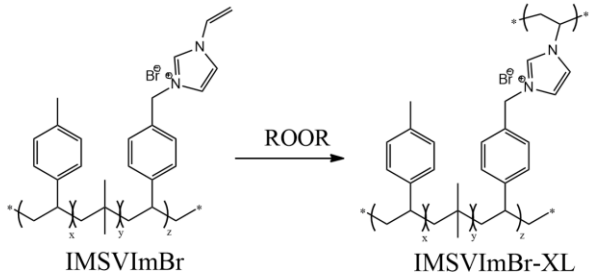

IMSVImBr IMSVImBr-XL

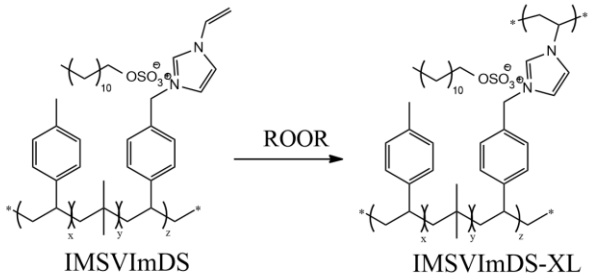

IMSVImDS IMSVImDS-XL

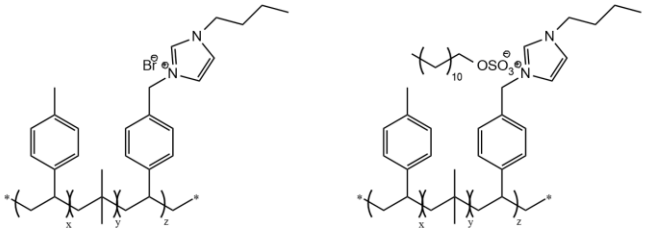

IMSBuImBr IMSBuImDS

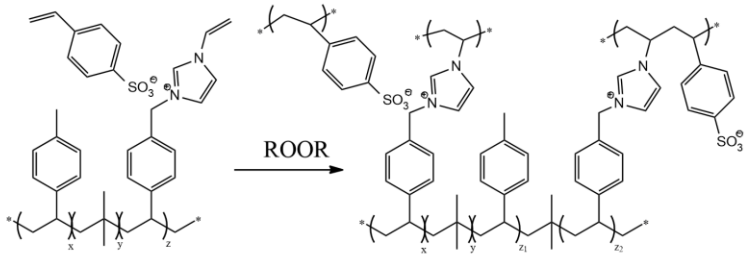

IMSVImSS IMSVImSS-XL

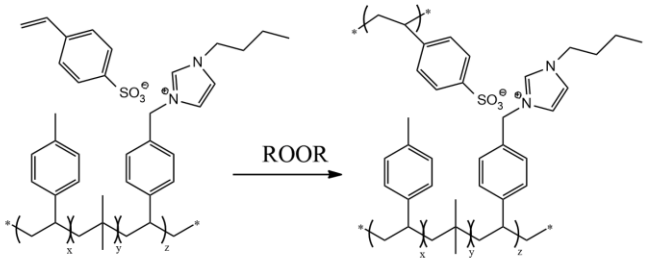

IMSBuImSS IMSBuImSS-DCP

3.3.1. Bromide versus dodecyl sulfate – thermoformable butylimidazolium ionomers

The 1-butyl-3-alkyl-imidazolium derivative of BIMS contains alkylimidazolium functionality that does not polymerize when heated with peroxide initiators. Since these ionomers do not contain a covalent network, chain entanglements and ionic aggregates are the only source of resistance to an imposed deformation. This accounts for the rather small storage modulus (Figure 3.1a) relative to conventional thermoset elastomers described in Chapter 2. The G' values recorded for the dodecyl sulfate butylimidazolium ionomer (IMSBuImDS) are notable in that they are significantly less than those of its bromide counterpart (IMSBuImBr). This suggests that the bulkier organic anion reduces the strength of ionic interactions that give rise to a high storage modulus. This is an important result, since rubber compounders generally dislike ionomeric elastomers because of their high viscosity. By exchanging bromide with dodecyl sulfate, one of the primary disadvantages of this technology can be mitigated.

The labile nature of ionic aggregates in IMSBuImBr and IMSBuImDS is revealed by a significant decline of G′ with temperature (Figure 3.1c), as well a unique loss tangent behavior in the 70-100ºC temperature range (Figure 3.1d). The tan δ sensitivity to temperature observed for both ionomers is evidence of an order-disorder transition that results from ionic network relaxation, and as expected, is lacking in the BIMS starting material.

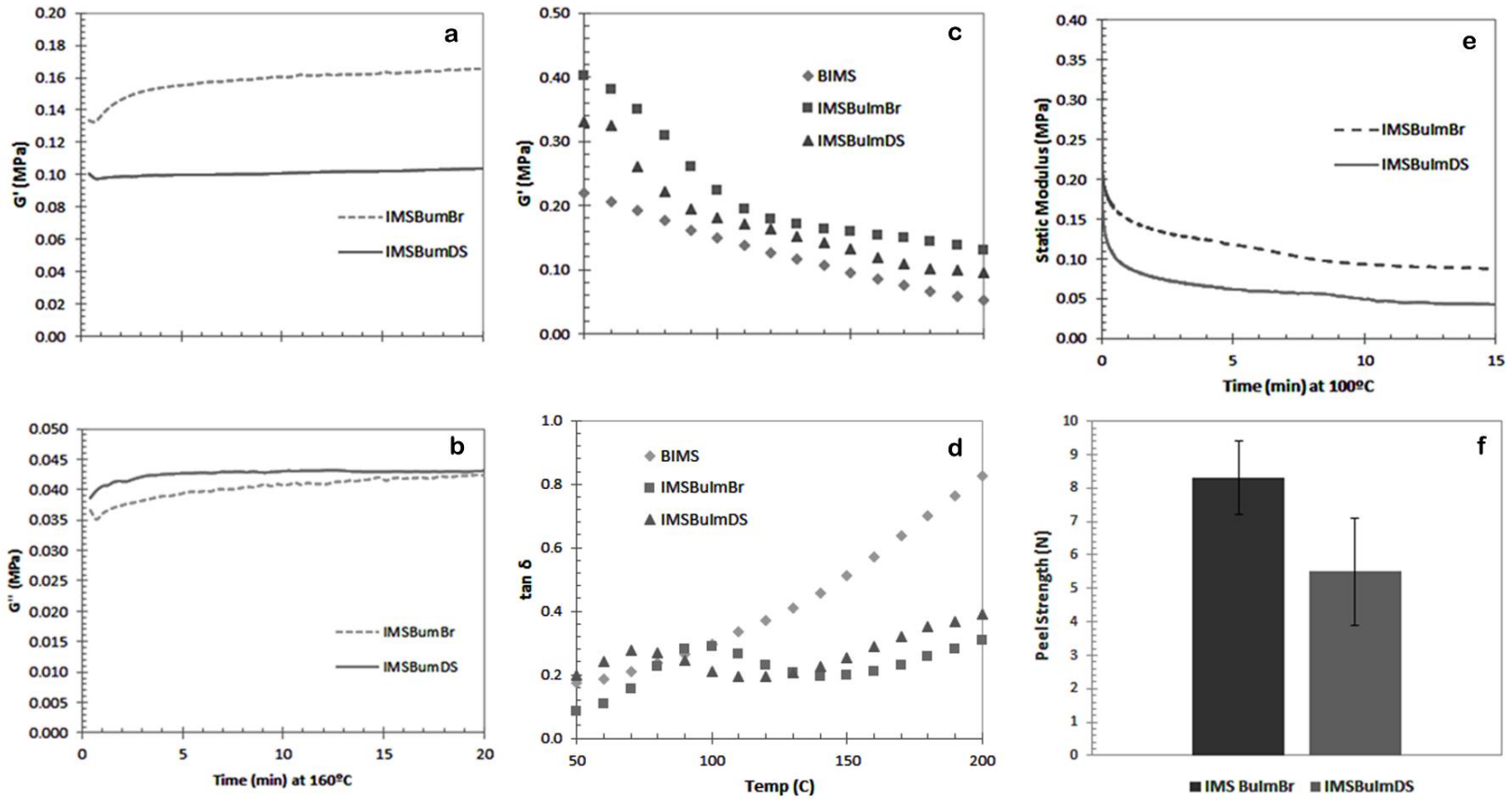

Figure 3.1. Storage modulus (a) and loss modulus (b) evolution with time at 160ºC (1Hz, 3º), storage modulus (c) and loss tangent (d) evolution with temperature, stress relaxation at 100 ºC (e) and peel strength (f) for IMSBuImBr and IMSBuImDS.

Multiple relaxation modes are frequently reported for other ionomer systems, and are identified by two peaks in their temperature sweep plots (Eisenberg & Navratil, 1973; Tsagaropoulos & Eisenberg, 1995). Typically, a low temperature process (β-relaxation) involves the onset of segmental motions within the polymer backbone, while a higher temperature process (α-relaxation) involves long-range motion of main and side chains due to the destabilization of the ionic network (Page, et al., 2005). In the present case, only one relaxation peak was observed between 50 and 100ºC, which could correspond to an α-relaxation where the ionic network is destabilized.

In the present context, the long-chain alkyl sulfate counter anion reduced the temperature at which the loss tangent relaxation peak appeared (Figure 3.d). Phillips and Moore found that when substituting sodium for tetrabutyl ammonium as the counter ion in perfluorosulfonate ionomers, relaxation peaks shifted to lower temperature due to a combined effect of reduction of electrostatic interactions within the ion aggregates, and the plasticization of the polymer backbone by the bulky alkylammonium groups (Phillips & Moore, 2006). Ionomers respond the same way to the introduction of surfactants (Tong & Bazuin, 1992), corroborating the hypothesis that bulky organic counter ions act as plasticizers.

Figure 3.1f provides a comparison of the peel strength data acquired for the uncured ionomer samples. Note that ionomers are generally valued for their adhesive properties, with the potential for ion pairs to interact with the permanent dipoles of materials such as nylon and siliceous fillers. The peel strength data suggests that the long chain aliphatic group within IMSBuImDS inhibits these functional group interactions. This issue is examined further in the next section dealing with crosslinked imidazolium ionomers.

The data presented to this point indicate that anion metathesis has a significant impact on rheological and adhesive properties. However, the data listed in Table 3.1 shows that exchanging bromide for dodecyl sulfate does not impact tensile properties significantly. Differences in Young's modulus values were not statistically significant, nor were the ultimate failure properties.

Table 3.1. Tensile properties of butylimidazolium ionomers of BIMS (150mm/min, 25ºC)

Polymer	Young's Modulus (MPa)	Stress at break (MPa)	Elongation at break (%)
IMS BuImBr	1.4 ± 0.2	3.59 ± 0.58	480 ± 71
IMS BuImDS	1.3 ± 0.1	3.97 ± 0.73	445 ± 73

3.3.2. Bromide versus dodecyl sulfate – thermoset vinylimidazolium ionomers

The influence of a long-chain alkyl sulfate counter anion in the peroxide-curable 1-vinyl-3-alkyl-imidazolium derivative of BIMS is demonstrated by the data provided in Figure 3.2. As seen in Figure 3.2a, the dodecyl sulfate ionomer had a lower initial storage modulus, consistent with observations on the thermoformable butylimidazolium materials described above. However, both ionomers provided a similar final storage modulus in their thermoset condition, meaning that dodecyl sulfate does not compromise the ultimate state of a peroxide cure.

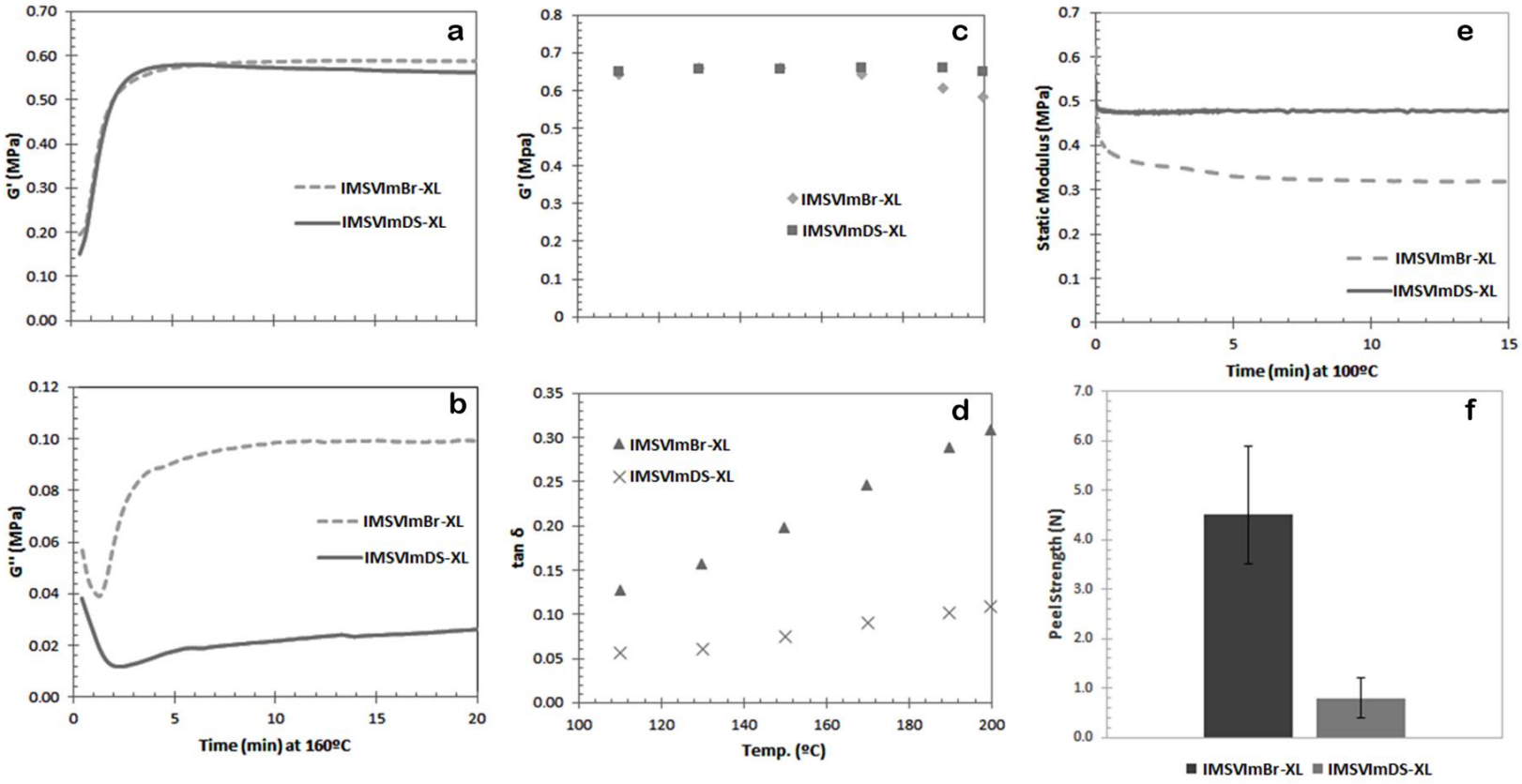

Figure 3.2. Storage modulus (a) and loss modulus (b) evolution with time at 160ºC (1Hz, 3º), storage modulus (c) and loss tangent (d) evolution with temperature, stress relaxation at 100 ºC (e) and peel strength (f) for IMSVImBr and IMSVImDS (18.5 µmol DCP/g)

Loss modulus data show that IMSVImBr and IMSVImDS behave differently during the curing process (Figure 3.2b). An initial decline of G" is expected, since covalent crosslinking reduces polymer segment mobility. However, the G" of IMSVImBr recovered over the following 10 min to exceed that of the uncured parent material, whereas the recovery observed for IMSVImDS was more subdued. The response of G" to hybrid ionic/covalent network formation is not well understood, making it difficult to speculate why this difference occurs. However, it is reasonable to assume that the aliphatic substituent of the dodecyl sulfate anion affects the strength of ion pair interactions as well as the ability of ion pairs to migrate amongst multiplets. The net result is an IMSVImDS-XL thermoset that is significantly more elastic than its IMSVImBr-XL analogue.

Figure 3.2c and Figure 3.2d summarize temperature sweep measurements for the IMSVImBr-XL and IMSVImDS-XL samples prepared by the crosslinking process illustrated in Figures 3.2a,b. Note that the thermal stability of the resulting networks is of considerable practical importance, particularly when a thermoset is used in severe service conditions. Although only data acquired during the heating cycle are plotted in Figure 3.2c and Figure 3.2d, the same values were recorded during a subsequent cooling cycle, indicative of good stability at 200ºC for short periods.

For covalent thermosets containing no ionic functionality, G' is expected to increase with temperature as the entropy-driven elasticity response becomes more intense (Gao & Weiner, 1992). In contrast, ionic networks show the opposite behavior since multiplets tend to relax with increased temperature. Both thermoset ionomers displayed a combination of these behaviours by demonstrating a G' that was temperature-insensitive, which is consistent with a hybrid covalent/ionic intermolecular network structure. However, loss tangent values of IMSVImDS-XL were considerably lower than those of IMSVImBr-XL, suggesting that the dodecyl sulfate counter

anion increases the elasticity of the ionomer at all the temperatures studied, not just at 160°C where the thermosets were prepared.

Figure 3.2e shows stress relaxation plots for IMSVImBr-XL and IMSVImDS-XL that demonstrate the improved resistance of the dodecyl sulfate thermoset to a constant strain deformation. Whereas IMSVImBr-XL lost 45% of its initial static modulus to relaxation of the ionic network, IMSVImDS-XL incurred a loss of just 13%. This constancy of the material`s response is important from an engineering application standpoint, as the thermoset is expected to better withstand a static load without incurring severe decline in restorative force.

Figure 3.2f illustrates the results of 180º peel strength tests, reported as the force needed to remove the cured ionomer from a Dartek nylon film. As observed for the butylimidazolium analogues, the organic anion caused a significant drop in adhesive strength, likely due to diminished interactions between polymer-bound ion pairs and the dipole moments of the nylon surface. Consistency between the thermoformable and thermoset ionomers was also observed in static tensile testing, as the properties of IMSVImBr-XL and IMSVImDS-XL were indistinguishable (Table 3.2). Note that the recorded elongations at break were lower than those required for many engineering applications, but tensile properties can be tuned using different proportions of peroxide-curable vinylimidazolium groups and unreactive butylimidazolium functionality (Ozvald, 2012). The higher the vinylimidazolium content, the greater the crosslink density of the peroxide-cured thermoset.

Table 3.2. Tensile properties of vinylimidazolium ionomers of BIMS (150mm/min, 25ºC)

Polymer	Young's Modulus (MPa)	Stress at break (MPa)	Elongation at break (%)
IMSVImBr-XL	4.4 ± 0.2	1.49 ± 0.17	36 ± 4
IMS VImDS-XL	4.7 ± 0.2	1.59 ± 0.05	36 ± 2

3.3.3. Bromide versus styrene sulfonate – thermoformable butylimidazolium ionomers

The recent development of peroxide curable ionomers was a significant advance in the field, allowing for thermoset elastomers with exceptional physical properties to be produced using relatively simple chemical syntheses. To date, the counter anions used in these materials have been unreactive (e.g. bromide, dodecyl sulfate), but the potential exists for unique materials to be prepared using anions bearing polymerizable functionality. To that end, 4-styrene sulfonate was selected as a counter anion, since it is known to copolymerize efficiently with 1-vinyl-3-alkyl-imidazolium cations (Jana, et al., 2013), and it can be homopolymerized to high yields by free radical chemistry (Men, et al., 2014).

A reactive dodecyl itaconic counter anion was susbtituted in the place of bromide on both, the butylimidazolium and vinylimidazolium ionomers of IMS. These ionomers were exposed to small amounts of peroxides at high temperatures and the final mechanical and physical properties did not differ in a significant way from those of the dodecyl sulfate ionomers reported before, indicating poor oligomerization of the counter anions.

Studies of the styrene sulfonate system began with an examination of butylimidazolium ionomers. The time sweep data presented in Figures 3.3a,b show how the storage and loss moduli

of IMSBuImSS change when compounded with 0.2 wt% peroxide and heated to 160°C to give its derivative, IMSBuIMSS-DCP. The large increase in storage modulus is particularly interesting, in light of the fact that the bromide analogue does not undergo peroxide-initiated crosslinking. Therefore, the radical oligomerization of styrene sulfonate counter anions must be responsible for the dramatic increase in elasticity.

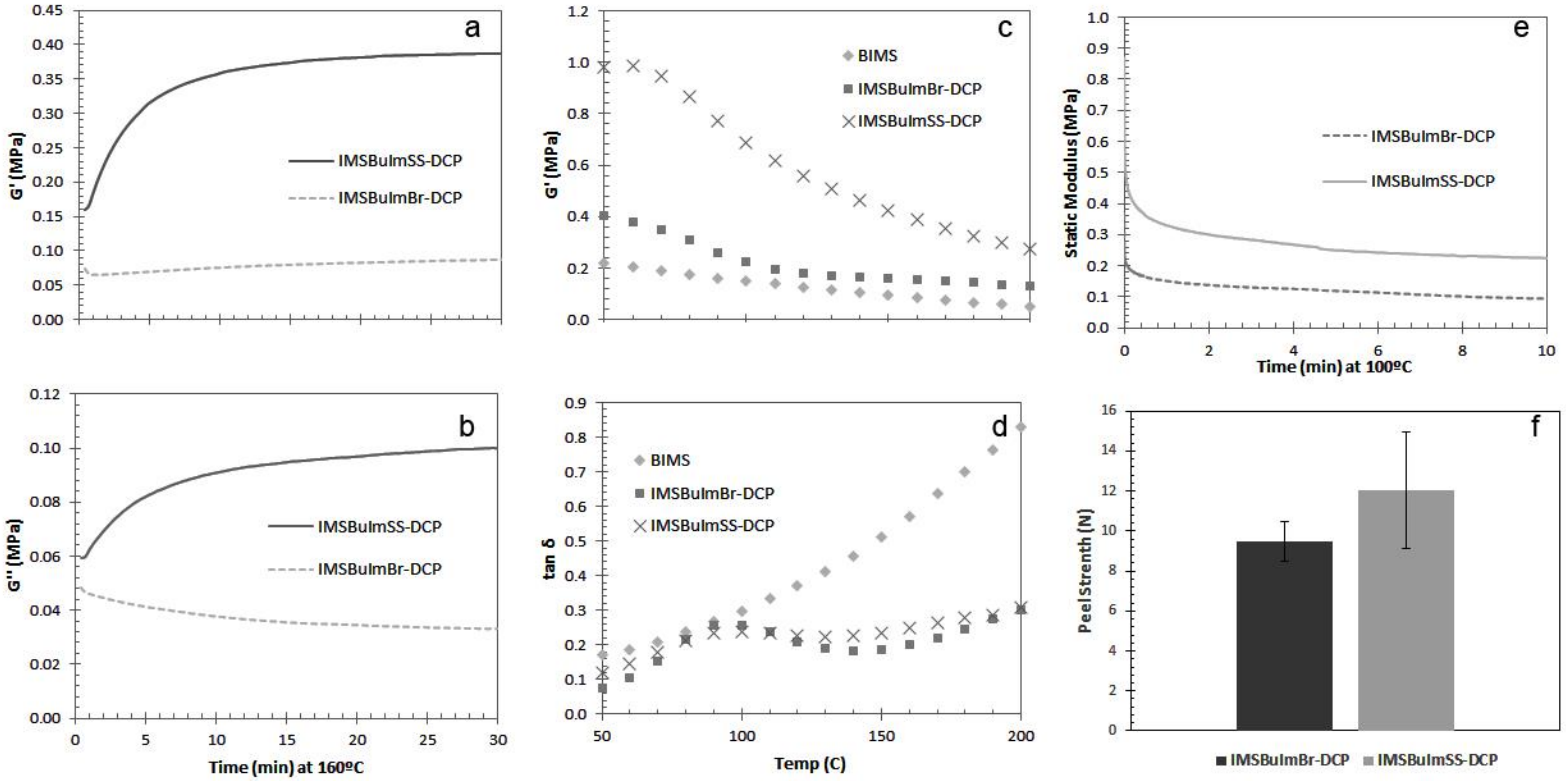

Figure 3.3. Storage modulus (a) and loss modulus (b) evolution with time at 160ºC, G' (c) and loss tangent (d) evolution with temperature, stress relaxation at 100 ºC (e) and stress-strain curve (f) for IMSBuImBr-DCP and IMSBuImSS-DCP (7.4 µmol DCP/g).

The effect of anion oligomerization on other material properties was equally dramatic. Figure 3.c and Figure 3.d show temperature sweeps for IMSBuImSS-DCP and IMSBuImBr-DCP, which demonstrate the higher storage modulus of the styrene sulfonate system at low temperature, but also a significant decline as the temperature was raised beyond 70°C. This behaviour is distinct from all the other materials presented in this thesis, in that a very high low temperature modulus, consistent with values observed for thermoset materials, diminished greatly with temperature, in keeping with a purely ionic network. Recall that covalent network strength increases with temperature, in direct opposition to the observed results.

Stress relaxation measurements (Figure 3.e) and static tensile data (Table 3.3) confirm that IMSBuImSS-DCP has a higher network density, with a physical properties that are, once again, consistent with a covalently crosslinked thermoset. Indeed, solubility tests showed that IMSBuImSS-DCP does not dissolve in chloroform, chloroform+tetrabutylammonium bromide, or toluene and toluene+hexanol, even when heated to reflux. Nevertheless, the material was thermoformable. It could be sheeted on a two-roll mill and compresson molded to give a solid plaque, whereas a material such as IMSVImBr-XL only produced crumb on the two-roll mill, and would not give a coalesced solid when heated in a compression mold.

Importantly, 180º peel strength test results were not significantly different between IMSBuImBr-DCP and IMSBuImSS-DCP (Figure 3.f). These results suggest that the styrene sulfonate counter anion does not diminish interactions between polymer-bound ion pairs and the dipole interactions of the surface of the nylon film, allowing for the manufacture of an elastic ionomeric material that preserves good adhesive properties. This is sharp contrast to the dodecyl sulfate system, in which severe losses in adhesive strength were observed.

Table 3.3. Tensile properties of butylimidazolium ionomers of IMSBuImBr and IMSBuImSS-DCP (150mm/min, 25ºC)

Polymer	Young's Modulus (MPa)	Stress at break (MPa)	Elongation at break (%)
IMS BuImBr	1.4 ± 0.2	3.59 ± 0.58	480 ± 71
IMS BuImSS-DCP	5.6 ± 0.6	8.42 ± 0.83	242 ± 49

3.3.4. Bromide versus styrene sulfonate – thermoset vinylimidazolium ionomers

An ionomer whose anionic and cationic functionality is capable of chemical reaction is a new composition of matter that might afford important engineering properties. If monomer copolymerization is significant, the resulting thermoset would be a polyampholyte, since both positive and negative charges would be polymer-bound. Physical property data for IMSVImBr-XL and IMSVImSS-XL are presented in Figure 3.4. The storage and loss modulus data plotted in Figure 3.4a,b show that peroxide activation of polymer-bound vinyl functionality and the reactive anion within IMSVImSS had the predictable outcome, with covalent crosslinking producing a stiffer, more elastic material. However, the most notable aspect of the IMSVImSS-XL data are their similarity to the unreactive sulfate anion material, IMSVImDS-XL (Figure 3.2). Both thermosets provide similar hybrid ionic/covalent network properties, and superior elasticity compared to the IMSVImBr-XL reference material.

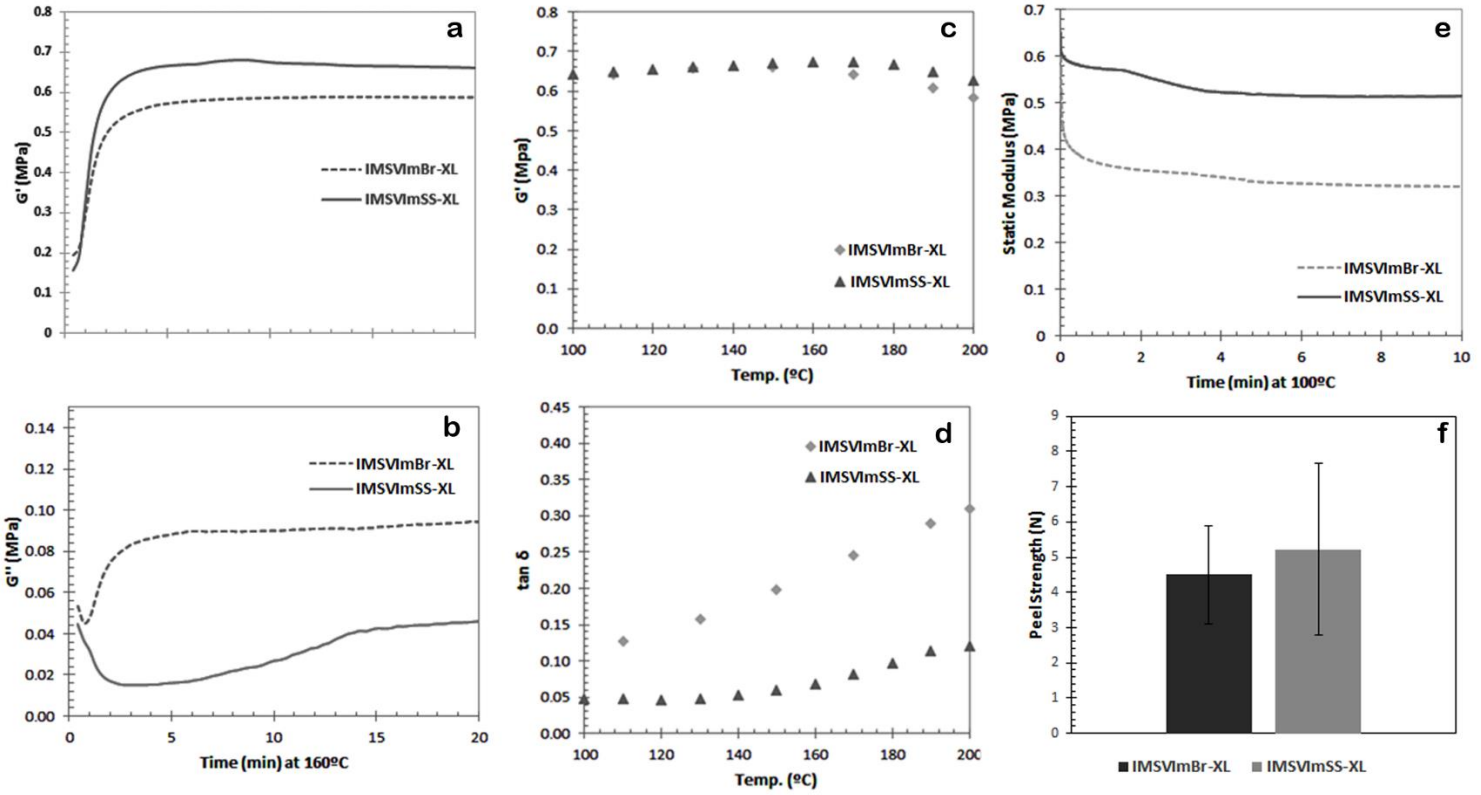

Figure 3.4. Storage modulus (a) and loss modulus (b) evolution with time at 160ºC (1Hz, 3º), storage modulus (c) and loss tangent (d) evolution with temperature, stress relaxation at 100 ºC (e) and stress-strain curve (f) for IMSVImBr and IMSVImSS (all ionomers were crosslinked using 18.5 µmol DCP/g).

The tensile modulus of IMSVImSS-XL is the highest observed in this study, and the failure properties are consistent with a tight covalent network that resists permanent deformation under a static load (Table 3.4). A key difference between IMSVImSS-XL and IMSVImDS-XL is adhesive strength. While the peal strength from a mylar film was just 0.8 N for the dodecyl sulfate thermoset, the value for the cured styrene sulfonate material was 5.3 N (Figure 3.4f), which is comparable to the bromide ionomer. Therefore, the styrene sulfonate system provides a unique combination of low uncured compound viscosity, high thermoset elasticity, and high adhesive strength. As such, the ion pair copolymerization concept may have commercial value.

Table 3.4. Tensile properties of vinylimidazolium ionomers of BIMS, IMSVImBr and IMSVImSS (150mm/min, 25ºC)

Polymer	Young's Modulus (MPa)	Stress at break (MPa)	Elongation at break (%)
IMS VImBr-XL	4.4 ± 0.2	1.49 ± 0.17	36 ± 4
IMS VImSS-XL	5.4 ± 0.3	1.87 ± 0.42	45 ± 11

3.4. Ionomer-clay nanocomposites

Polymer-layered silicate nanocomposites (PLSNs) are a class of materials in which nanometer scale layered silicates are dispersed into an organic polymer matrix. They generally provide mechanical and barrier properties that are better than their unfilled parent materials, and often outperform conventional composites that are reinforced by micron-scale fillers. The most common layered silicates used in the manufacture of PLSNs belong to the familiy of 2:1 layered phyllosilicates, consisting of two tetrahedrally coordinated silicon atoms forming a octahedral sheet of either aluminum or magnesium hydroxide. Isomorphic substitution within the layers generates

negative forces that are counterbalance by alkali and alkaline earth cations situated in the interlayer space.

Two main characteristics of layered silicates make them suitable for the production of nanocomposites; their ability to disperse into individual platelets of nanoscale-size dimension, and the ability to tune their surface chemistry through ion exchange with organic and inorganic cations. The number of exchangable cations per dry weight unit of clay is defined as the cation exchange capacity (CEC) and it is an inherit characteristic of each type of clay. Montomorillonite, hectorite and saponite (Table 3.) are three of the most used 2:1 phyllosilicates in the manufacture of polymer-clay nanocomposites.

Table 3.5. Nomenclature, chemical formula and cation exchange capacity (CEC) of commonly used 2:1 phyllosilicates

Clay nomenclature	Chemical Formula	CEC (mequiv/100g)
Montmorillonite	$Mx(Al_4\text{-}Mg_x)Si_8O_{20}(OH)_4$	110
Hectorite	$Mx(Mg_{6\text{-}x}Li_x)Si_8O_{20}(OH)_4$	120
Saponite	$MxMg_6(Si_8\text{-}Al_x)Si_8O_{20}(OH)_4$	86.6

In this section, the possibility of exchanging the alkali cations in the interlayer of sodium montmorillonite with polymer-bound imidazolium functionality is explored. The vinylimidazolium thermosets described above failed at relatively low elongations, typically less than 50%, which is problematic for studies of filler reinforcement. Therefore, the ionomer prepared for this stage of the study was a mixed alkylation product, IMSMImBr, containing 0.115 mmole butyl imidazolium / gram polymer and 0.115 mmole vinylimidazolium /g polymer. Reducing the concentration of

peroxide-curable functionality lowers the covalent network density, thereby increasing tensile failure properties to the extent that is needed for assessing the degree of filler reinforcement.

Dispersion of montmorillonite into the polymer matrix

The intercalation of montmorillonite was achieved by mixing a dispersion of 4.4 g of sodium montmorillonite in 25 mL of DMSO with a solution of 40 g of IMSMImBr in 500 mL of toluene. A similar method to intercalate organic clays on BIMS has been previously reported in literature (Maiti, et al., 2004). The resulting polymer-clay nanocomposite solution was emulsified with water to generate a driving force for anion metathesis by dissolving NaBr in the aqueous phase. Anion exchange was confirmed qualitatively using the silver nitrate method on the aqueous phase that was isolated after precipitation of the polymer from solution.

The extent of clay exfoliation and clay dispersion was determined by means of wide angle X-ray diffraction (XRD) and further corroborated by Transmission Electron Microscopy (TEM). When using XRD, clay intercalation is evidenced by the reduction of the angle of incidence (2Θ) for the diffraction peak corresponding to the silicate interlayer spacing. The unmodified sodium montmorillonite clay gave 2Θ = 6.0º, while the value observed for the IMSMImBr composite gave 2Θ = 5.1º (Figure 3.5). This reduction in interlayer spacing between clay platelets (d_{hkl}) is consistent with a high degree of intercalation, since these variables are inversely proportional as stated in Bragg's Law (equation 3.1).

$$d_{hkl} = \frac{n\,\lambda}{2\sin\theta} \qquad (3.1)$$

A high degree of clay exfoliation was achieved by processing the intercalated polymer nanocomposite at 80ºC in a two-roll-mill. The exfoliation of the clay into dispersed platelets is

evidenced by the decrease of the intensity of the 5.0º peak as the number of passes through the mill increased from zero up to 10 and 20 cycles (Figure 3.).

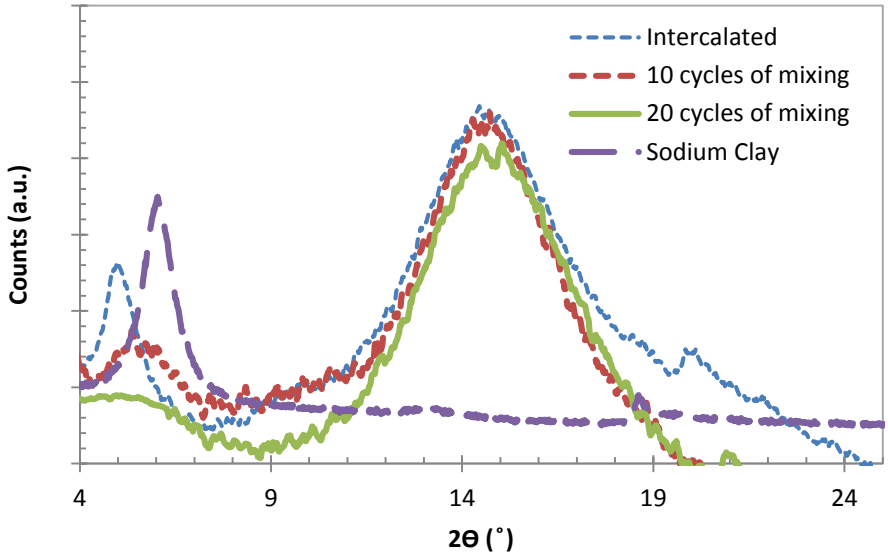

Figure 3.5. XRD spectra for the IMSMImBr polymer-clay nanocomposites at different stages of the manufacturing process

The extent of clay exfoliation and platelet dispersion was further assessed by TEM. Figure 3.6 shows images of the ionomer nanocomposite prepared by the emulsion-based metathesis and milling procedures described above, and a control sample prepared by passing IMSMImBr + clay through the mill 20 times at 80°C. The TEM images of the anion-exchanged sample (Figure 3.6a and Figure 3.6c) show smaller clay aggregates and better platelet dispersion compared to the control sample (Figure 3.6b and Figure 3.6d). As such, the exchanged material can be classified as a nanocomposite, since its filler particle size is on the nanometer scale.

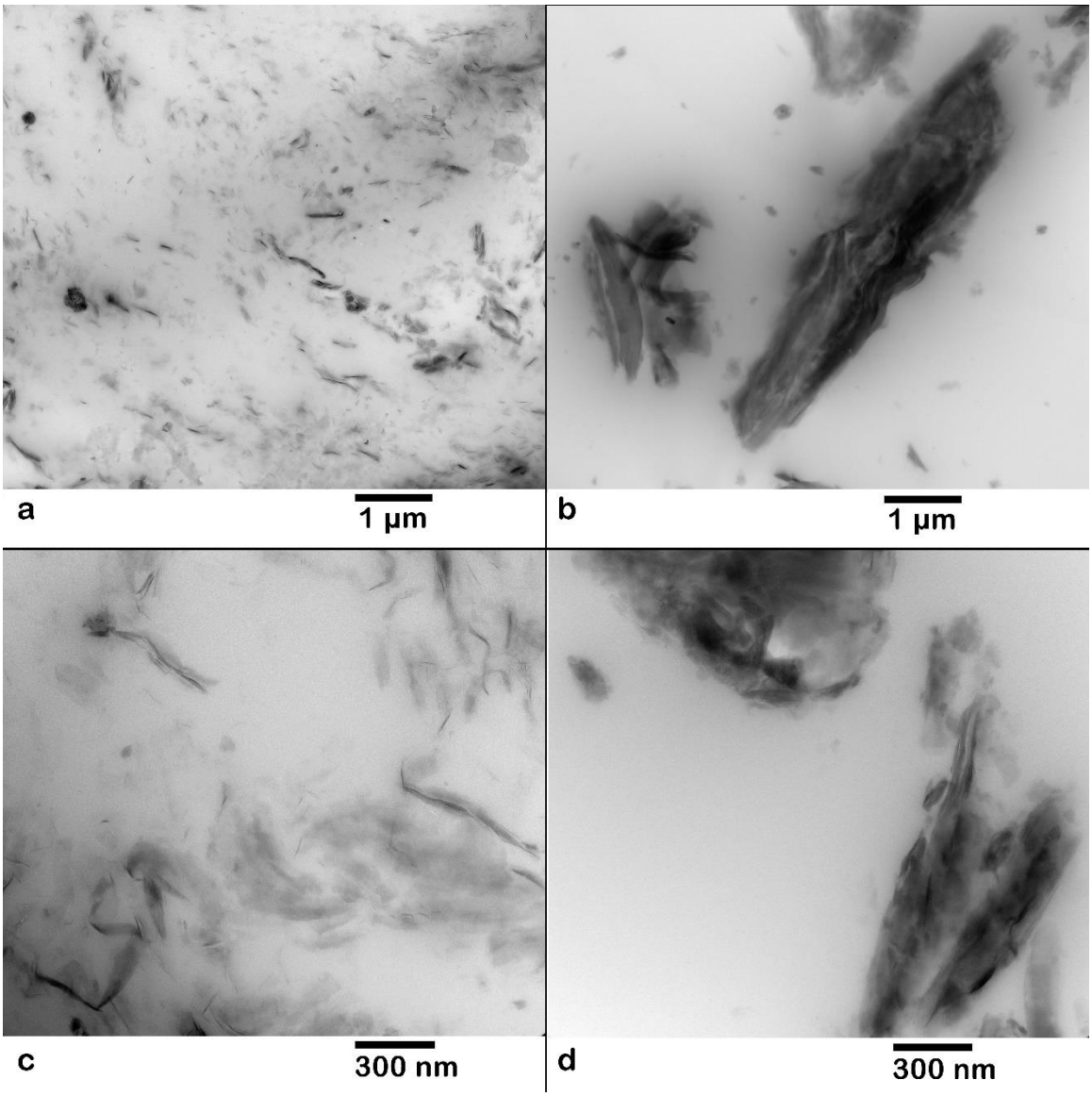

Figure 3.6. TEM images of IMSMImBr 10% wt. clay manufactured through (a,c) solvent blending + mechanical mixing and (b,d) mechanical mixing alone.

The impact of exfoliated clay on cure dynamics and thermoset material properties is illustrated in Figure 3.7, where the nanocomposite is compared directly with unfilled IMSMImBr. The clay did not affect peroxide curing dynamics, but it did reinforce the thermoset material significantly, raising the final dynamic storage modulus by 42% (from G'=0.38 to G'= 0.54 MPa,

Figure 3.7a) and the loss modulus by 150% (from G”= 0.02 to G”= 0.05 MPa, Figure 3.7b). Note that filler reinforcement generally raises the loss modulus of a thermoset elastomer, and the magnitude of the observed G” increase is consistent with other filled systems. The temperature sweep and stress relaxation data (Figure 3.7c,d) are unremarkable, apart from the greater stiffness observed for the nanocomposite in each test.

The tensile data illustrated in Figure 3.7f and summarized in Table 3.6 demonstrate the extent to which 10% wt. montmorillonite can reinforce the ionomer when it is exfoliated and dispersed. The Young’s Modulus was improved by 36% over the unfilled ionomer thermoset, and the ultimate stress at break was raised by 184% without compromising the maximum elongation. These results are notable in that such a small filler loading can enhance thermoset properties.

Table 3.6. Static tensile data for clay-reinforced and unfilled ionomer thermosets.

Sample	Young's Modulus (MPa)	Stress at break (MPa)	Elongation at break (%)
IMSMImBr unfilled	4.8 ± 0.1	1.9 ± 0.2	53 ± 11
IMSMImBr 10% wt. clay	6.5 ± 0.3	5.4 ± 0.5	63 ± 8

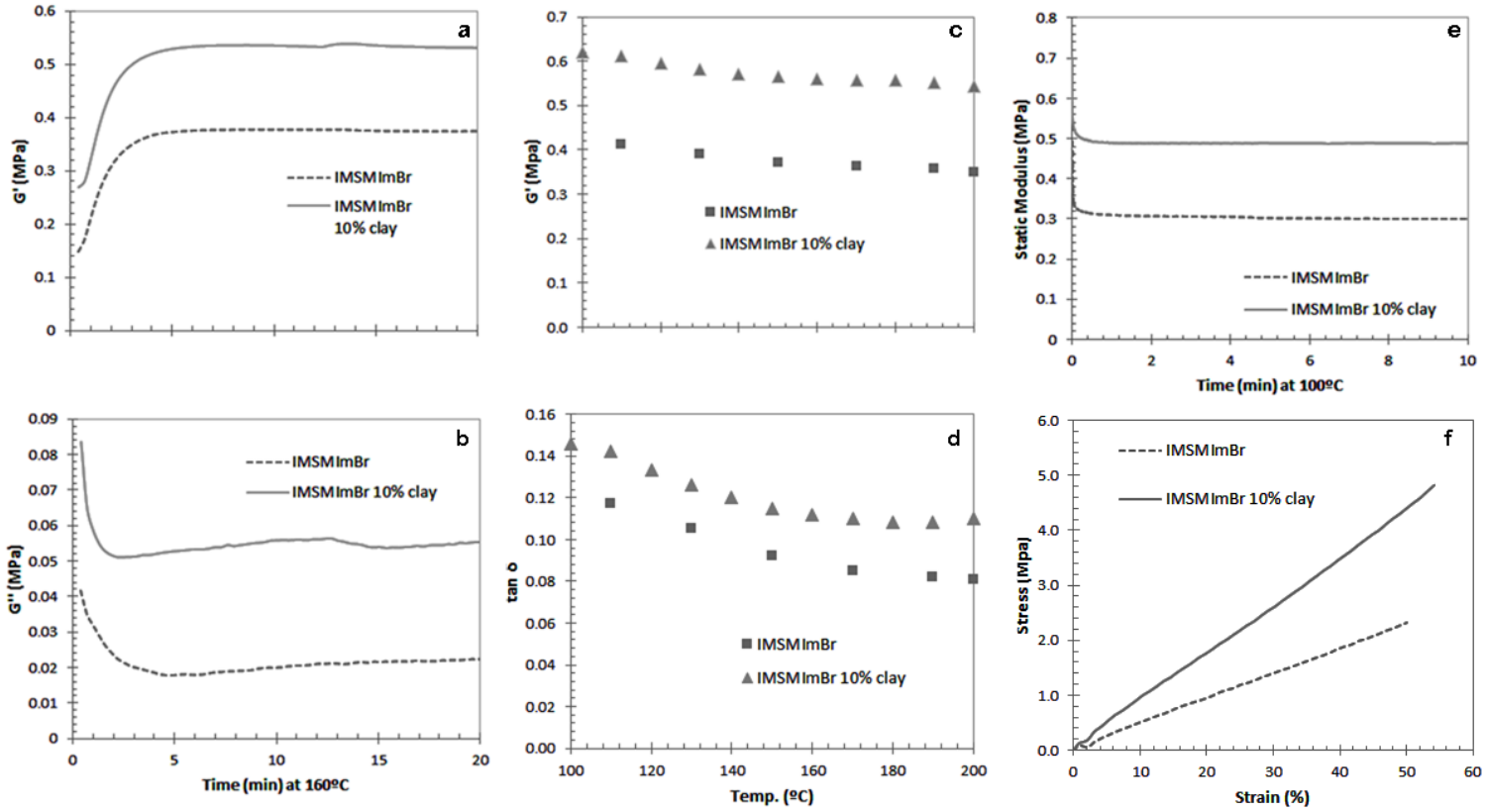

Figure 3.7. Storage modulus (a) and loss modulus (c) evolution with time at 160ºC (1Hz, 3º), storage modulus (c) and loss tangent (d) evolution with temperature, stress relaxation at 100 ºC (e) and stress-strain curve (f) for IMSMImBr/10% clay nanocomposites cured with 0.5% wt. DCP compared to the unfilled thermoset.

3.5.Conclusions

A series of counter anions have been introduced to vinylimidazolium and butylimidazolium ionomers derived from BIMS. Results demonstrate that the type of counter anion has a significant effect on multiplet formation and stability. The dodecyl sulfate counter anion reduces the viscosity of the uncrosslinked ionomer while improving elasticity of the crosslinked thermoset. This may have significant implications for ionomer processability, since high viscosity is a main concern of rubber compounders. However, the weakened ion pair interactions that underlie these improvements come at the cost of reduced adhesive strength.

The polymerization of styrene sulfonate counter anions seems to increase crosslink density on the vinylimidazolium ionomers, reducing the contribution of the ionic network towards the formation of a more pure covalent thermoset than in the case of the pure bromide vinylimidazolium ionomer. The introduction of these same polymerizable counter anions in a butylimidazolium ionomer of BIMS increases the storage modulus of the elastomers once it has been treated with small amounts of peroxide at high temperatures, but the ionic network still relaxed under applied load, proving the predominance of intermolecular ion pair interactions.

The exfoliation of anionic clay platelets by associating with cationic imidazolium ionomers gives rise to significant improvements in dynamic shear properties as well as static tensile properties. These benefits are realized using comparatively low filler loadings, and without incurring complications in peroxide cure dynamics and yields.

3.6. Works Cited

Arjunan, P., Wang, H. & Olkusz, J., 1998. *New options via chemical modification of polyolefins: Part 1. Synthesis and properties of novel phosphonium ionomers from poly(isobutylene-co-bromomethylstyrene),* s.l.: Functional Polymers, American Chemical Society Symposium Series.

Eisenberg, A. & Navratil, M., 1973. Ion clustering and viscoelastic relaxation in styrene-based ionomers. II Efect of ion concentration. *Macromolecules,* 6(4), pp. 604-612.

Feldheim, D. L., Lawson, D. R. & Martin, C. R., 1993. Influence of the sulfonate countercation on the thermal stability of Nafion perfluorosulfonate membranes. *Journal of polymer science Part B: polymer physics,* Volume 31, pp. 953-957.

Gao, J. & Weiner, J. H., 1992. Range of validity of the entropic spring concept in polymer melt relaxation. *Macromolecules,* Volume 25, pp. 3462-3467.

Hirasawa, E., Yamamoto, Y., Tadano, K. & Yano, S., 1991. Effect of the metal cation type on the structure and properties of ethylene ionomes. *Journal of Applied Polymer Science,* Volume 42, pp. 351-362.

Jana, S., Vasantha, V. A., Stubbs, L. P. & Parthiban, A., 2013. Vinylimidazole-based asymmetric ion pair comonomers: synthesis, polymerization studies and formation of ionically crosslinked PMMA. *Journal of Polymer Chemistry,* 51(15), pp. 3260-3273.

Kumar, D. K., Gupta, S., Tsou, A. H. & Bhowmick, A. K., 2008. Compatibility and viscoelastic properties of brominated isobutylene-co-p-methylstyrene rubber/tackifier blends. *Journal of Applied Polymer Science,* 10(3), pp. 1485-1497.

Maiti, M., Sadhu, S. & Bhowmick, A. K., 2004. Brominated poly(isobutylene-co-para-methylstyrene) (BIMS)-clay nanocomposites: Synthesis and characterization. *Journal of polymer science Part B: polymer physics,* 42(24), pp. 4489-4502.

Men, Y., Schlaad, H., Voelkel, A. & Yuan, J., 2014. Thermoresponsive poymerized gemini dicationic ionic liquid. *Polymer Chemistry,* Volume 5, pp. 3719-3724.

Ozvald, A. M., 2012. Reactive ionomers: N-vinylimidazolium bromide derivatives of poly(isobutylene-co-isoprene) and poly(isobutyle-co-para-methylstyrene). *Unpublished Manuscript, Queen's University.*

Page, K. A., Cable, K. M. & Moore, R. B., 2005. Molecular origins of the thermal transitions and dynamic mechanical relaxation in perfluorosulfonate ionomers.. *Macromolecules,* 38(15), pp. 6472-6484.

Parent, J. S., Malmberg, S. M. & Whitney, R. A., 2011. Auto-catalytic chemistry for the solvent-free synthesis of isobutylene-rich ionomers. *Green Chemistry,* Volume 13, pp. 2818-2824.

Parent, J. S., White, G. D. & Whitney, R. A., 2002. Amine Substitution Reactions of Brominated Poly(isobutylene-co-isoprene): New Chemical Modification and Cure Chemistry. *Macromolecules,* Volume 35, pp. 3374-4479.

Phillips, A. K. & Moore, R. B., 2006. Mechanical and transport property modifications of perfluorosulfonate ionomer membranes prepared with mixed organic and inorganic counterions. *Jounral of Polymer Science. Part B: Polymer Physics.,* 44(16).

Tong, X. & Bazuin, G. C., 1992. Plasticization of a poly(ethyl acrylate) ionomer by an alkyl amine. *Journal of Polymer Science. Part B: Polymer Physics,* 30(4).

Tsagaropoulos, G. & Eisenberg, A., 1995. Direct observation of two glass transitions in silica-filled polymers. Implications for the morphology of random ionomers.. *Macromolecules,* Volume 28, pp. 396-398.

Tsou, A. H., Duvdevani, I. & Pawan, A. K., 2004. Quaternay ammonium elastomeric ionomers by melt-state conversion. *Polymer,* 45(10), pp. 3163-3173.

Wang, H. C., Fusco, J. V. & Hous, P., 1994. Acrylate ester modifications of isobutylene-paramethylstyrene copolymer. *Rubber World,* pp. 37-41.

Weiss, R. A., Agarwal, P. K. & Lundberg, R. D., 1984. Control of ionic interactions in sulfonated polystyrene ionomers by the use of alkyl-substituted ammonium counterions. *Journal of applied polymer science,* Volume 29, pp. 2719-2734.

Chapter 4

Conclusions and Future Recommendations

Conclusions

BIIR-derived macro-monomers

The terminal carboxylic group on the itaconic functionality provides a reactive position for the addition of further functionalities. This approach was explored by synthesizing an itaconic derivative bearing an aminoanthraquinoyl chromophoric group and grafting it on IMS. The resulting polymer crosslinked in the presence of peroxide while displaying a coloring similar in terms of absorption to the original dye. Additionally, an itaconic derivative bearing an aminosiloxane group was prepared and grafted on IIR, producing a polymer that displayed improved dispersion of silica.

However, the modification of the itaconic group proved to have certain limitations since the formation of terminal esters or amides seems to affect cure performance of the macro-monomer.

BIMS-derived ionomers

The N-alkylation of imidazolium functional groups on BIMS produces ionomers that display some of the typical characteristics of this particular type of polymers, such as high Young's Modulus and high viscosity. Two series of imidazolium derivatives of BIMS were prepared in order to explore the impact of anion metathesis on the final properties of the ionomer; a group of reactive ionomers based on 1-vinylimidazole to explore the response of different crosslinked ionomers to anion metathesis and another group based on 1-butylimidazole to analyze the behavior of the uncured ionomeric elastomers.

The exchange of bromine for a long-chain alkyl sulfate as counter anion increased the cure yield of the crosslinked ionomer while decreasing the viscosity of the uncrosslinked elastomer, characteristics that improve the processability and performance of the final product. The introduction of polymerizable counter anions resulted in an overall increase in elasticity in both the crosslinked and uncrosslinked ionomer. Additionally, the cationic nature of the ionomer proved to offer an advantage in stablishing interactions between the polymer matrix and clay fillers, resulting in a considerably increase in elastic performance of the resulting nanocomposite.

Recommendations for future work

Future work in the BIIR macro-monomer field should focus on analyzing in depth the properties of the synthesized peroxide crosslinkable macro-monomers, with a special focus on their dynamic mechanical properties and thermal stability, including their propensity to hydrolysis at high temperatures. In case it was found that the stability of the macro-monomers in question was compromised in the presence of moisture, the possibility of N-alkylation of BIIR to synthesize peroxide crosslinkable macro-monomers should be examined.

Regarding the functionalization of the itaconic group, the formation of an amide on the terminal carboxylic position of the itaconic group has proven to reduce its cure yield. Therefore, the functionalization of this group through esterification has to be explored in order to assess if the behavior is the same in that case. Likewise, since it has been found that the nature of the terminal group can affect crosslinking performance of the itaconic functionality, the introduction of activating groups could help improve its crosslink yield.

Regarding the ionomeric derivatives of BIMS, further analysis are needed to understand more in depth the structure and behavior of the ionic network. The introduction of counter anions

with transition metals would facilitate determination of multiplet size via SAXS and performing thermal mechanical analysis in a wider range of temperatures would allow us to observe the impact of different counter anions on the behavior of the ionic network at lower temperatures.

Lastly, the influence of counter anion size on mechanical and physical properties of the ionomer should be evaluated. Ionomers bearing counter anions of different sizes may display a wide range of properties between pure ionic polymers and their non-ionic counterparts and therefore, the specific properties of the ionomer could be engineered and tuned to target specific applications. Additionally, the disparity in adhesion properties found between ionomers bearing different counter anions prove the decisive role of ionic groups on surface properties. Since adhesion is one of the attractive properties of ionomers, the impact of counter anion size on adhesion should be evaluated.

Appendix A

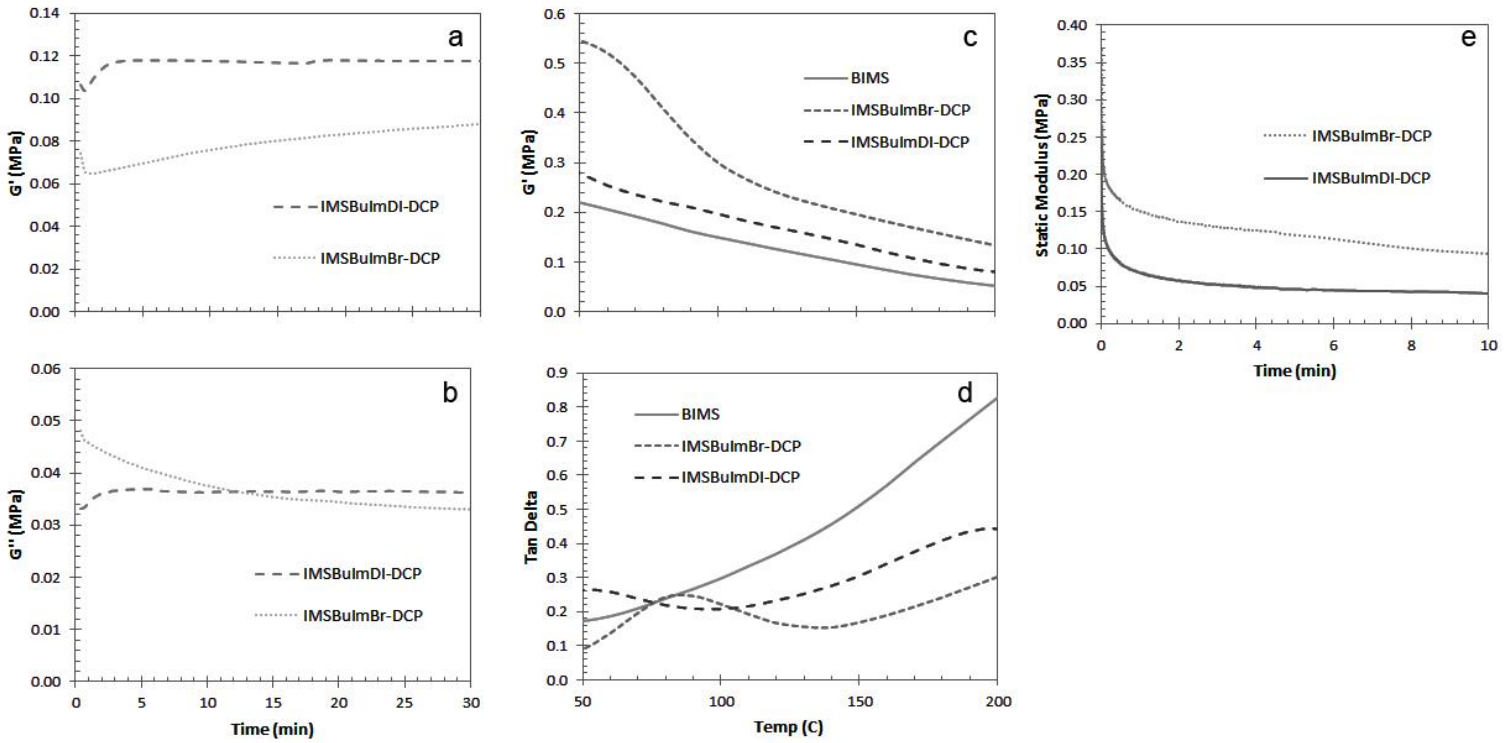

Figure A.1. Storage modulus (a) and loss modulus (b) evolution with time at 160ºC, G' (c) and loss tangent (d) evolution with temperature and stress relaxation at 100 ºC (e) for IMSBuImBr-DCP and IMSBuImDI-DCP (7.4 µmol DCP/g).

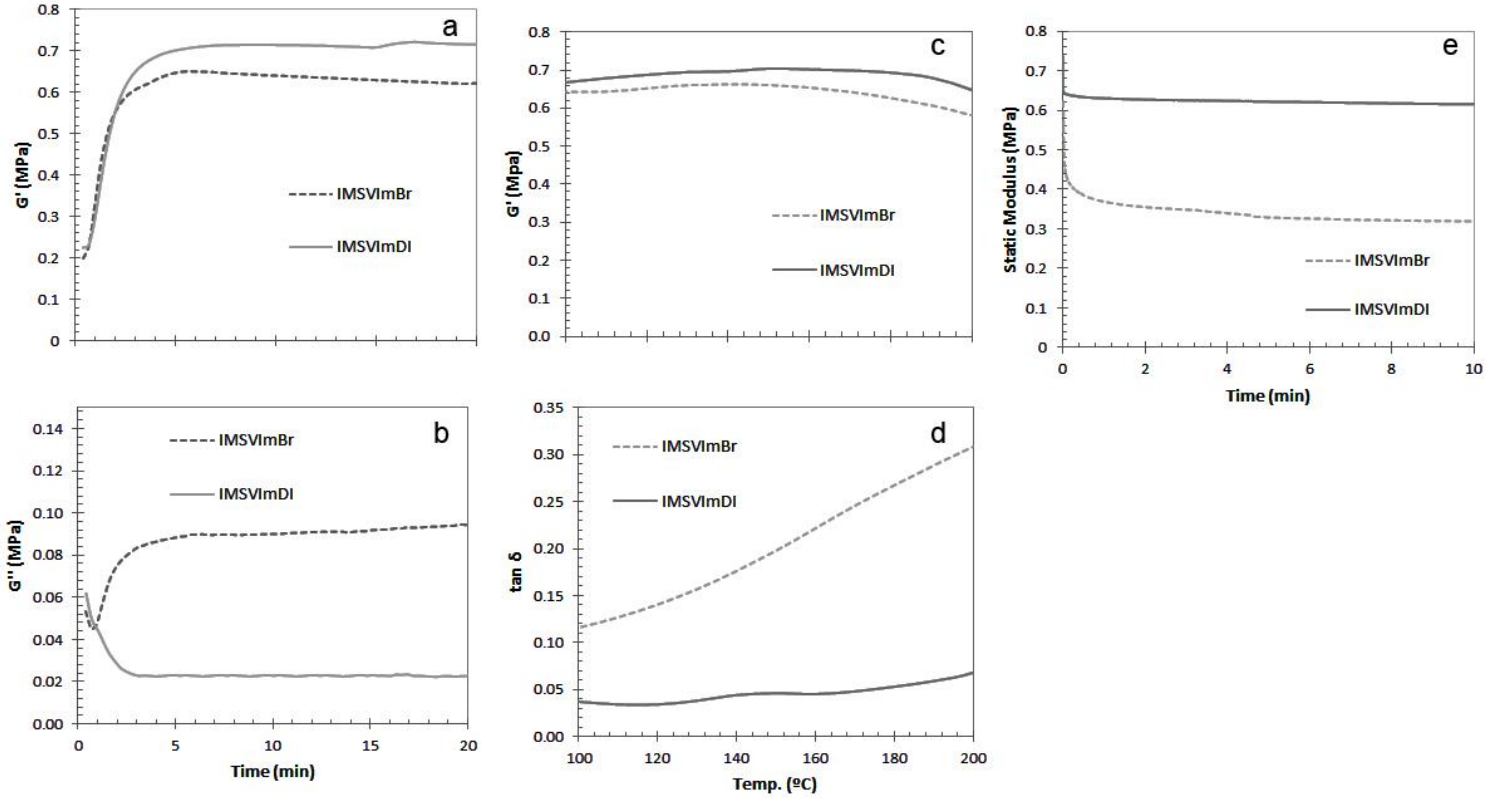

Figure A.2. Storage modulus (a) and loss modulus (b) evolution with time at 160ºC (1Hz, 3º), storage modulus (c) and loss tangent (d) evolution with temperature and stress relaxation at 100 ºC (e) for IMSVImBr and IMSVImDI (all ionomers were crosslinked using 18.5 µmol DCP/g).